Centre for Population Ageing Research (CEPAR)

Working Paper 2026/03

Prudential Liquidity Rules beyond Banking: Evidence from Refundable Deposit Funding for Residential Care Providers

Lingfeng Lyu, Michael Sherris, Francesco Ungolo, Zhiqian Ye

Prudential Liquidity Rules beyond Banking: Evidence from Refundable Deposit Funding for Residential Care Providers

Lingfeng Lyu[1,2], Michael Sherris[1,2], Francesco Ungolo[1,2], Zhiqian Ye[1,2]

[1]School of Risk and Actuarial Studies, UNSW Sydney, NSW 2052, Australia.
[2]Centre for Population Ageing Research (CEPAR), UNSW Sydney, NSW 2052, Australia.

Abstract

While the structural mismatch between illiquid assets and demandable liabilities is a source of fragility in traditional banking, this capital–liquidity tradeoff is migrating to the non-banking sector, emerging as a vulnerability in the global aged care industry. Unlike traditional banks, aged care providers are highly exposed to demographic and mortality shocks. A crisis such as the COVID-19 pandemic can reduce occupancy, depressing operating cash flows and triggering large-scale refunds of deposit-like accommodation balances. Using Australia's newly introduced Minimum Liquidity Amount (MLA) regulation as a prime empirical setting, this paper evaluates rigid, one-size-fits-all liquidity buffers against forward-looking, stress-based frameworks. We develop a stochastic simulation model that integrates resident flows with macroeconomic conditions and provider balance-sheet dynamics, utilising a continuous-time Markov chain. The analysis of representative providers reveals that the uniform application of the default MLA misaligns with true liquidity risk profiles: it imposes excessive regulatory constraints on larger providers while remaining insufficiently stringent for smaller ones. To address these limitations, a risk-sensitive MLA framework is proposed, calibrated via a multidimensional stress testing procedure which replicates the regime shifts induced by exogenous shocks. Expressed as a linear, balance-sheet-based rule, the risk-sensitive framework preserves crisis resilience while expanding the capital–liquidity frontier across the aged care sector. By integrating stress-test-based foundations within a transparent rule, it offers a transferable template for prudential regulation beyond the banking perimeter.

Keywords: Aged care regulation; Liquidity risk; Minimum Liquidity Amount; Capital formation; Refundable deposits; Stress testing.

JEL classification: G28, G32, G01, C63, I18, J14

1 Introduction

Managing the structural mismatch between illiquid capital investments and demandable, deposit-like liabilities remains a fundamental prudential challenge. While this capital–liquidity tradeoff has been extensively analysed within the traditional banking sector (Acharya et al., 2011; Cornett et al., 2011; Davydov et al., 2021), this fragility is rapidly migrating to the non-bank sector, where it has emerged as a distinct vulnerability in the expanding global aged care industry. In several major ageing economies, including Australia, parts of the United States, and segments of the Japanese for-profit market, care providers rely on deposit-like refundable accommodation funding to finance capital assets such as real estate and infrastructure.

Unlike the depositor-run-driven fragility analysed by Diamond and Dybvig (1983) and Goldstein and Pauzner (2005), liquidity outflows in the aged care sector are dictated by stochastic events like mortality and resident turnover. This intersection of demographic risk and classical corporate finance frictions generates structural vulnerabilities distinct from those in banking. Because care providers rely on inherently illiquid assets, their true resilience hinges on the critical wedge between gross asset value and actual pledgeability (Holmström and Tirole, 1998). Unexpected spikes in refund demands therefore risk triggering severe fire-sale discounts (Brunnermeier and Pedersen, 2009) and binding collateral constraints (Donaldson et al., 2020). These latent frictions are acutely exposed during system-wide crises. Recent years provided an example of a dual shock, where the COVID-19 pandemic destabilised demographic flows while subsequent monetary tightening eroded asset values (Jiang et al., 2024). Despite the severity of this conjunction between demographic run risk and macro-financial tightening, the finance literature lacks a quantitative framework to evaluate optimal liquidity buffers for non-bank entities operating in such dynamic environments.

To address this gap, we use the Australian aged care sector as our empirical laboratory. Its market for refundable accommodation deposits generates significant liquidity risks within a non-banking setting, and its regulatory regime offers a prototypical example of a one-size-fits-all approach. In 2025, the Aged Care Quality and Safety Commission (ACQSC) proposed a Minimum Liquidity Amount (MLA), compelling providers to hold liquidity based on a rigid and backward-looking formula (ACQSC, 2025). We refer to this baseline regulatory standard as the default MLA (dMLA). This proposal represents the government's response to the systemic shock of the COVID-19 pandemic, yet it relies heavily on an inflexible, "Basel I-style" methodology (Cummings and Durrani, 2016). Drawing a parallel with the banking sector highlights this regulatory lag. While banks responded to the Global Financial Crisis by evolving toward the risk-sensitive compromises of Basel III/IV, the aged care sector entered the pandemic without a comparable history of regulatory maturation. To evaluate whether such prescriptive rules adequately capture true liquidity risk, we develop a stochastic simulation framework that jointly models macroeconomic conditions, resident flows, and balance-sheet dynamics.

Drawing on representative provider archetypes, we show that the dMLA misaligns with true liquidity risk in two opposing directions. For large, well-capitalised providers, the dMLA overconstrains capital formation: holdings below the dMLA do not necessarily signal liquidity distress. Conversely, for smaller, less-diversified providers, the dMLA is insufficient, leaving them under-buffered against

genuine liquidity risk. To address this distortion, we propose a risk-sensitive alternative (rMLA) calibrated via a multidimensional stress test. By anchoring required buffers directly to provider-specific balance-sheet values, the rMLA expands the capital–liquidity frontier for well-capitalised providers while tightening it where genuine fragility exists. For a representative large provider, the rMLA unlocks up to AUD 223 million (a 27% increase) in investment capacity, while holding the probability of a liquidity crunch below 1% under severe stress across all archetypes.

The contribution of this paper is three-fold. First, we develop a tractable, queueing-based framework that extends demographic modelling to a prudential regulatory setting, enabling joint simulation of demographic and macroeconomic shocks on resident-driven refundable liabilities. Second, we propose a methodology that projects the output of complex stochastic stress tests onto a transparent, rule-based liquidity formula. The resulting rMLA inherits the transparency of a fixed buffer while integrating provider-specific risk-bearing capacity through observable balance-sheet characteristics. Third, from a policy perspective, we show that the rMLA improves the capital–liquidity tradeoff by aligning required buffers with each provider's risk-bearing capacity. Because sector-wide risk in aged care is driven by exogenous shocks rather than the endogenous financial contagion documented in banking (Sydow et al., 2024), the rMLA reverses standard banking prescriptions (Acosta-Smith et al., 2026) by tightening requirements for small providers and relaxing them for large ones. This reversal reframes the conceptual relationship between aged-care and banking prudential design.

The remainder of the paper is organised as follows. Section 2 outlines the prudential landscape, while Sections 3 and 4 detail the simulation framework and its calibration. Section 5 evaluates the risk-sensitive MLA, with policy implications in Section 6 and concluding remarks in Section 7.

2 Prudential regulation landscape

This section first details the Australian aged care sector's funding structure and the dMLA, and then contrasts this regulation with the prudential standards of traditional finance and comparable international aged care sectors.

2.1 Institutional setting and the MLA framework

Australian aged care providers employ dual-segment business models, encompassing both residential aged care facilities (RACFs) and retirement villages (RVs). RACF residents finance their accommodation through a lump-sum refundable accommodation (RA) channel, an equivalent non-refundable daily accommodation (DA) channel, or a combination thereof.[1][2] The RV segment operates a parallel refundable contribution structure, in which residents' upfront entrance payments are returned upon departure subject to tenure-dependent retention. Together with the RA channel, this funding

[1] For self-funded RACF residents, these payments are formally termed Refundable Accommodation Deposits (RAD) and Daily Accommodation Payments (DAP); for partially government-supported residents, they are Refundable Accommodation Contributions (RAC) and Daily Accommodation Contributions (DAC). For analytical tractability, we aggregate these instruments into RA and DA, respectively.

[2] For analytical tractability, our framework assumes a strict bifurcation between these channels, treating residents as belonging entirely to either the RA or DA channel.

model exposes providers to deposit-like outflows whose timing is governed by demographic rather than financial events.

Despite differences in the demographic profiles of the RACF and RV segments, their liquidity frictions are intrinsically linked at the provider level. While governed by different demographic and financial parameters, the RA and RV channels are structurally isomorphic in their refund mechanics. To regulate these provider-wide liquidity risks, the dMLA imposes a one-size-fits-all buffer that aggregates exposures across the provider's entire operations (ACQSC, 2025). Specifically, as illustrated in Figure 1, this buffer comprises three components: 35% of the provider's prior-quarter core cash outflows, 10% of RA liabilities, and 2% of refundable RV liabilities.

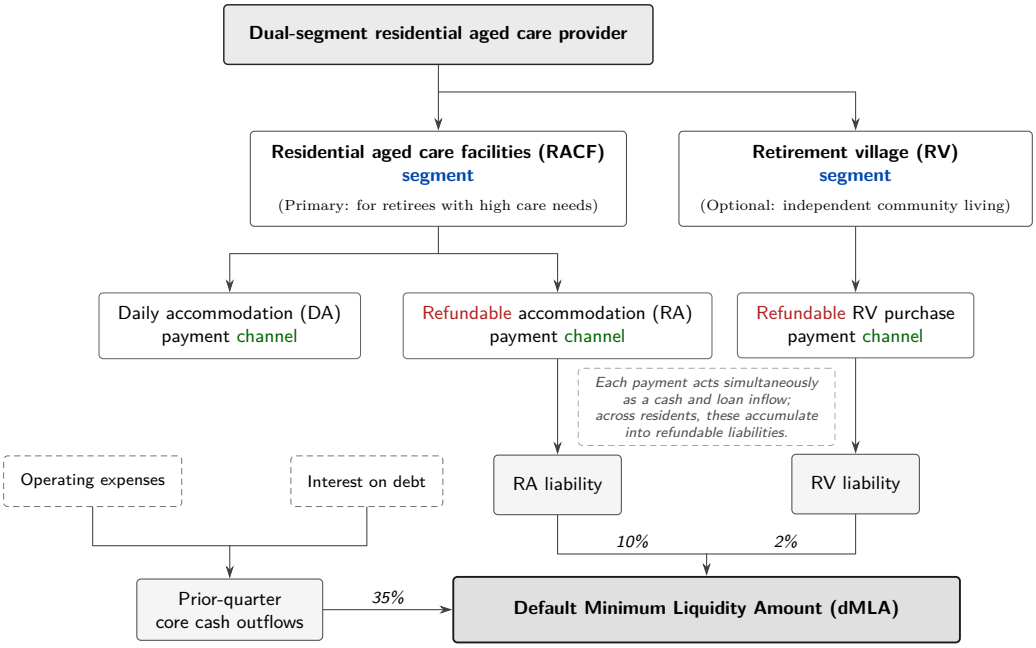

Figure 1. Composition of the default Minimum Liquidity Amount (dMLA) across segments and funding channels. The RV segment is called 'optional', reflecting the reality that some providers do not have this segment.

2.2 Comparative landscape of prudential liquidity regulation

To contextualise the MLA framework, Table 1 compares prudential liquidity regulations across sectors and jurisdictions. The comparison highlights a regulatory shortcoming: while the underlying liquidity risks in global aged care are driven by demographic shocks, prevailing regulatory instruments remain deterministic. This structural mismatch between dynamic risks and static rules is evident not only in Australia's dMLA, but also in U.S. operating reserves and Japanese trust fund guarantees.

By contrast, entities supervised by the Australian Prudential Regulation Authority (APRA) manage analogous liquidity risks through stochastic stress testing and scenario analysis. The structural parallels between aged care providers and these regulated entities motivate the development of a suitable risk-sensitive and transparent prudential framework for the sector.

Table 1. Prudential treatment of deposit-like refundable liabilities: a cross-sectoral and cross-jurisdictional comparison

Sector	Framework / standard	Structural similarity to the baseline	Structural difference from the baseline	Prudential metric	Stochastic modelling
Panel A: Baseline — Australian aged care					
Aged care providers	ACQSC guidance[a]	—	—	dMLA	No
Panel B: Australian financial sector regulated by APRA.					
Banks	APS 210	Maturity mismatch between demandable, deposit-like liabilities and illiquid assets.	Outflows arising from run-driven fragility and rollover risks rather than demographic events.	Liquidity Coverage Ratio; Net Stable Funding Ratio; supervisory stress testing	Hybrid[b]
Private health insurers	HPS 110; HPS 231	Stochastic cash outflows driven by health and demographic factors.	Outflows arise as insurance claims rather than deposit refunds.	Prescribed Capital Amount; scenario analysis	Yes
Superannuation (Australia's defined contribution pension)	SPS 530; SPG 530	Member-driven outflows are uncertain, analogous to resident-driven refund demands.	Outflows blend behavioural fund switching with preservation-age and retirement withdrawals.	Liquidity stress testing across multiple horizons	Yes
Panel C: International aged care					
United States[c]	State-level licensure; statutory operating reserves	Funding combines partially refundable upfront entrance fees with ongoing service payments.	Prudential requirements are set at the state level and vary substantially across jurisdictions.	Operating reserve calibrated to estimated operating costs	No
Japan[d]	Escrow accounts, trust, and guarantees	Partially refundable entrance fees are a material liability in the for-profit segment.	Protection operates ex post at the level of individual deposits rather than through a holistic balance-sheet buffer.	No prescribed metric; provider-level contractual safeguards	No

Notes: This table characterises the prudential treatment of deposit-like refundable liabilities across sectors and jurisdictions, using Australian aged care (Panel A) as the baseline. All APRA prudential standards are contained in APRA (2026).

[a] Our analysis focuses exclusively on the dMLA. Although the regulatory framework theoretically permits an evaluated MLA alternative (ACQSC, 2025), it is devoid of actionable implementation guidelines. Consequently, it operates primarily as a qualitative compliance exemption rather than a systematic, risk-sensitive prudential mechanism.

[b] Consistent with global banking standards: Basel III/IV establish a hybrid framework via an output floor, mandating that stochastic capital models yield no less than 72.5% of the standardised fixed requirement (Cummings and Durrani, 2016).

[c] The funding structure is documented in Zarem (2010), and operating-reserve requirements are discussed in Pearson (2006).

[d] Institutional features and the external protection mechanisms used for refundable entrance fees are described in Aveline-Dubach (2022) and Sakurai (2017).

3 Simulation framework for liquidity and capital dynamics

This section describes the forward-looking simulation model used to evaluate the tradeoffs between liquidity and capital formation faced by aged care providers over a one-year simulation horizon.[3]

3.1 Overview

The simulation framework considers the following four components:

Macroeconomic conditions (Section 3.2). Nominal interest rates, inflation, and the cost of debt are treated as exogenous variables. These variables determine the real discount rate and the indexation of operating cash flows.

Balance-sheet dynamics (Section 3.3). The balance-sheet items are grouped as liquid assets, capital assets, trade receivables, financial liabilities, and refundable liabilities. The simulation model specifies how each component evolves over the simulation horizon, which is specific to the provider's underlying cash flow dynamics and liquidity management strategies.

Cash flow dynamics (Section 3.4). Resident admissions, departures, and length of stay are assumed to follow a capacity-constrained continuous-time Markov chain. In combination with the macroeconomic conditions, these resident-flow dynamics determine government subsidies, resident-funded daily fees, refundable contributions, operating expenditures, and refund obligations.

Liquidity management and prudential regulation (Section 3.5). Providers respond to liquidity surpluses or shortfalls according to a stylised liquidity management rule. To evaluate a provider's financial fragility under stress, we measure (i) the probability of a liquidity crunch and (ii) the probability of breaching the applicable liquidity requirement. This framework aligns our analysis with the stress-testing methodologies standard in APRA-regulated sectors (see Table 1).

3.2 Macroeconomic conditions

3.2.1 Interest rate and inflation dynamics

The macroeconomic conditions are described through the nominal risk-free rate $r(t)$ and the inflation rate $\pi(t)$. The joint process $(r(t), \pi(t))$ is assumed to follow a vector autoregression (VAR) model (Sims, 1980). These variables are used to discount and index the operating cash flows of aged care providers.

[3] While resident liabilities can span a decade or more, the one-year horizon reflects the core objective of prudential liquidity buffers: absorbing acute, short-term stress. These buffers are designed to prevent immediate provider failure and limit the government's contingent liability during sudden systemic shocks, as illustrated by Australia's 2021–2022 post-pandemic period, rather than to dictate multi-year capital structures.

3.2.2 Real vs nominal quantities

All monetary quantities in the model, including balance-sheet items and cash flows, are expressed in real terms. Hence, the expected present values are computed using the real short rate, denoted as $r^{\text{real}}(t)$, implied by $(r(t), \pi(t))$ at time t:

$$r^{\text{real}}(t) = \frac{1 + r(t)}{1 + \pi(t)} - 1. \tag{1}$$

Accordingly, the real investment return $r^{\text{inv}}(t)$ and the real long-term borrowing cost $r^{\text{debt}}(t)$, are derived by deflating their respective nominal counterparts by inflation:

$$1 + r^{\text{inv}}(t) = \frac{1 + r(t) + \delta_1}{1 + \pi(t)}; \quad 1 + r^{\text{debt}}(t) = \frac{1 + r(t) + \delta_2}{1 + \pi(t)}, \tag{2}$$

where δ_1 denotes the contractual spread earned on short-term liquid placements (e.g., term deposits) over the risk-free rate. This spread reflects the baseline counterparty credit risk and funding costs of the commercial banking sector, instead of the broader market risk (Cornett et al., 2011). Similarly, δ_2 is a term-spread parameter calibrated such that the implied nominal borrowing rate, $r(t)+\delta_2$, matches the observed long-term funding cost for the provider, proxied by the mortgage rate benchmark.

3.3 Balance-sheet dynamics

To begin, we discretise the one-year horizon into intervals of length Δt, such that $T = 1/\Delta t$ periods are analysed. State variables evaluated at time t represent their beginning-of-period values and are assumed to remain constant over the interval $[t,\ t + \Delta t)$.

3.3.1 Asset and liability itemisation

In the simulation framework, the provider's balance sheet is itemised with a focus on liquidity and funding sources. Total assets are defined as $X(t) = X^i(t) + X^l(t)$, where $X^l(t)$ represents liquid assets and $X^i(t)$ represents illiquid assets (further comprising capital assets $X^c(t)$ and illiquid trade receivables $X^r(t)$). Correspondingly, total liabilities are expressed as: $L(t) = L^s(t)+L^l(t)+L^{\text{RV}}(t)+L^{\text{RA}}(t)$, comprising short-term ($L^s(t)$) and long-term ($L^l(t)$) financial liabilities, alongside liabilities arising from retirement villages ($L^{\text{RV}}(t)$) and refundable accommodation deposits ($L^{\text{RA}}(t)$). Both of these refundable balances (L^{RV} and L^{RA}) function similarly to callable funding: outflows are triggered by resident departures and are therefore event-driven rather than maturity-driven. Table 2 outlines the structural decomposition of a provider's balance sheet at time t.

3.3.2 Evolution of the balance sheet over time

We next characterise the balance-sheet dynamics governing the joint evolution of assets and liabilities to analyse the evolution of a provider's financial position over time. Because notation introduced here recurs throughout the framework, Table 3 consolidates key symbols for reference.

Table 2. Balance-sheet components in the modelling framework.

Category	Notation	Description & Assumption	Example
Panel A: Assets			
Liquid assets	$X^l(t)$	Assets that can be readily used to meet operating obligations and liquidity buffer requirements.	Current assets: cash, deposits, near-cash receivables due within one month, etc.
Capital assets	$X^c(t)$	Long-lived assets used in service provision and typically not realisable at short notice. *Model assumption: extracting liquidity from these assets at short notice is captured by the leverage-sensitive emergency borrowing premium in Equation (9).*	Non-current assets: property, equipment, long-term intercompany receivables, etc.
Trade receivables	$X^r(t)$	Outstanding amounts owed to the provider but not yet received in cash. These are treated as illiquid because collection is subject to delay.	Trade receivables (external) aged beyond one month.
Panel B: Liabilities			
Short-term financial liabilities	$L^s(t)$	Borrowings and financial obligations due within a short horizon. *Model assumption: all providers are assumed to share a common repayment horizon in the baseline specification; sensitivity analysis follows.*	Short-term loans and bridging finance (emergency borrowing collateralised by capital assets), etc.
Long-term financial liabilities	$L^l(t)$	Borrowings with longer maturities used to finance persistent investment needs. *Model assumption: providers share a common repayment horizon, and no new long-term debt is issued during the simulation.*	Loans used for property acquisition, redevelopment, or facility expansion.
RV liability	$L^{\mathrm{RV}}(t)$	Liabilities arising from refundable purchase payments linked to the retirement village segment.	RV balances repayable when residents leave.
RA liability	$L^{\mathrm{RA}}(t)$	Liabilities arising from refundable accommodation payments linked to the RACF segment.	RA balances repayable when residents leave.

Table 3. Key notation used in the simulation framework (excluding those defined in Table 2).

Notation	Description	First Eq.	Section
Panel A: Macroeconomic and pricing			
$r(t), \pi(t)$	Nominal risk-free rate and inflation rate	(1)	3.2
$r^{\mathrm{inv}}(t)$	Real return on liquid investments	(2)	3.2
$r^{\mathrm{debt}}(t)$	Real long-term borrowing rate	(2)	3.2
ϕ_1, ϕ_2	Emergency-borrowing intercept and leverage loading	(9)	3.3
Panel B: Cash flow components over $[t, t+\Delta t)$			
$\Delta L^i_{\mathrm{new}}(t)$	New short/long-term borrowing, $i \in \{s, l\}$	(7)	3.3
$\Delta L^k_{\mathrm{ret}}(t)$	Refundable retention deduction, $k \in \{\mathrm{RA}, \mathrm{RV}\}$	(10)	3.3
$\Delta I^{\mathrm{gov}}(t)$	Government subsidies	(13)	3.4
$\Delta I^{\mathrm{ind}}(t)$	Individual resident fees	(14)	3.4

Continued on next page.

Table 3 continued from previous page.

Notation	Description	First eq.	Section
$\Delta I_k^{\text{in}}(t)$	RA/RV refundable inflow, $k \in \{\text{RA}, \text{RV}\}$	(15)	3.4
$\Delta O^{\text{oprt}}(t)$	Operating expenses	(16)	3.4
$\Delta O^{\text{repay}}(t)$	Debt servicing (interest plus principal)	(17)	3.4
$\Delta O_k^{\text{out}}(t)$	Refund outflow on resident departure, $k \in \{\text{RA}, \text{RV}\}$	(18)	3.4
Panel C: Resident-flow (See Appendix A for more details)			
λ, ν	Post-shock admission intensity and departure hazard	—	3.4
V	Facility maximum capacity	—	3.4
ℓ	Elapsed length of stay (LOS) of a resident	—	3.4
$f^{\text{in}}(\ell; t)$	Snapshot LOS density of residents present at time t	—	3.4
$g(\ell)$	Refund schedule as a function of elapsed LOS	—	3.4
$N^{\text{RACF}}(t), N^{\text{RV}}(t)$	Resident census in RACF and RV segments	(13)	3.4
$\Delta A(t), \Delta D(t)$	Admissions and departures over $[t, t + \Delta t)$	(15)	3.4
Panel D: Operational and contractual parameters			
ψ_1, ψ_2, γ	Settlement-delay probabilities and receivable realisation rate	(5)	3.3
F^{gov}	Annual government subsidy per RACF resident	(13)	3.4
P_{DA}	Annual daily accommodation charge per RACF resident	(14)	3.4
$F^{\text{RACF}}, F^{\text{RV}}$	Annual per-resident fee in RACF and RV	(14)	3.4
P_k^{in}	Upfront loan amount per new resident, $k \in \{\text{RA}, \text{RV}\}$	(15)	3.4
$\theta_{\text{RA}}, \theta_{\text{DA}}$	RACF resident shares choosing RA/DA channels	(15)	3.4
$O^{\text{cost}}, O^{\text{other}}$	Per-resident and fixed operating cost	(16)	3.4
Panel E: Liquidity management and prudential variables			
κ	Capital expenditure (CAPEX) investment rate	(3)	3.3
$\mathcal{T}_M$	Set of quarterly MLA inspection times	(19)	3.5
LR_t	Applicable liquidity requirement at time t	(19)	3.5

Notes: The table lists the principal symbols throughout the simulation framework. Additional auxiliary parameters defined locally to a single equation are not repeated here. To clarify the distinction between institutional segments (RACF vs. RV) and their corresponding funding channels (RA, DA, and RV), please refer to Figure 1.

Capital assets. Let LR_t denote the applicable liquidity requirement at time t (formally specified in Section 3.5):

$$X^c(t + \Delta t) = X^c(t) + \kappa\big(X^l(t) - \text{LR}_t\big)^+. \tag{3}$$

When liquid assets exceed LR_t, we assume that a fraction $\kappa \in [0, 1]$ of the surplus is allocated to capital expenditure (CAPEX).

Liquid assets. Accounting for the capital expenditure, the dynamics of the liquid assets can be obtained as follows:

$$X^l(t + \Delta t) = X^l(t)(1 + r^{\text{inv}}(t))^{\Delta t} + \Delta I(t) - \Delta O(t) - \kappa\big(X^l(t) - \text{LR}_t\big)^+, \tag{4}$$

where $\Delta I(t)$ and $\Delta O(t)$ denote respectively aggregate cash inflows and outflows.

Trade receivables. To track the evolution of trade receivables, we net out the cash recovered from existing claims and add the delayed portions of newly accrued revenues. Let $\Delta I^{\text{gov}}(t)$ and $\Delta I^{\text{ind}}(t)$ denote the actual cash inflows received from government subsidies and resident contributions over the interval $[t, t+\Delta t)$. Because these cash inflows capture only the settled fraction $(1-\psi)$ of the total accrued revenue, we explicitly scale them by $\frac{\psi}{1-\psi}$ to quantify the unsettled amounts. By incorporating the settlement delay probabilities (ψ_1 and ψ_2) and the conditional realisation rate (γ), we model the dynamics of trade receivables as:

$$X^r(t+\Delta t) = (1-\gamma\Delta t)\, X^r(t) + \frac{\psi_1 \Delta I^{\text{gov}}(t)}{1-\psi_1} + \frac{\psi_2 \Delta I^{\text{ind}}(t)}{1-\psi_2}. \tag{5}$$

Remark 3.1 (Settlement delays and the reform shift)**.** *Under the pre-reform baseline, the government settles subsidies within one period (Δt). Thus, $\psi_1 = 0$, and providers accumulate no aged receivables from this source. The proposed reforms, however, require residents to replace a proportion $\tilde{\psi}$ of these government subsidies with their own contributions. We assume this shifted funding inherits the residents' standard settlement delay, yielding an effective delay rate of $\psi_1 = \tilde{\psi}\psi_2$ for this revenue.*

Remark 3.2 (Realisation of aged receivables)**.** *We model the resident payment settlement lag, τ, as an exponentially distributed random variable, $\tau \sim \text{Exp}(\mu_0)$, where the rate parameter $\mu_0 > 0$ governs the constant hazard rate of settlement. Consequently, the probability that the resident payment becomes trade receivable is*

$$\psi_2 = \Pr(\tau > \Delta t) = e^{-\mu_0 \Delta t}.$$

To determine how quickly these receivables convert to cash in subsequent periods, we use the exponential distribution's memoryless property. This property yields a constant conditional realisation rate, γ:

$$\gamma = \frac{\Pr(\tau \le 2\Delta t \mid \tau > \Delta t)}{\Delta t} = \frac{1 - e^{-\mu_0 \Delta t}}{\Delta t}. \tag{6}$$

Financial liabilities. We assume short-term liabilities amortise over a horizon shorter than one year:

$$L^s(t+\Delta t) = L^s(t) - \Delta L^s_{\text{repay}}(t) + \Delta L^s_{\text{new}}(t), \tag{7}$$

where $\Delta L^s_{\text{repay}}(t)$ denotes the scheduled repayment of principal, and $\Delta L^s_{\text{new}}(t)$ is the emergency borrowing the provider undertakes to bridge liquidity gaps relative to the liquidity requirement LR_t. Long-term liabilities are those with maturity greater than one year. For the purposes of the simulation model, we assume that there is no new issue over the simulation horizon:

$$L^l(t+\Delta t) = L^l(t) - \Delta L^l_{\text{repay}}(t). \tag{8}$$

Remark 3.3 (Emergency borrowing)**.** *We assume that emergency borrowing (i.e., the new short-term borrowing) scales with the liquidity shortfall according to*

$$\Delta L^s_{\text{new}}(t) = \left(\text{LR}_t - X^l(t)\right)^+ \exp\!\left(\phi_1 + \phi_2 \frac{L(t)}{X(t)}\right), \tag{9}$$

where $\phi_1 < 0$ shifts the baseline funding multiplier below unity in unstressed conditions; $\phi_2 > 0$ scales the additional cost imposed by higher leverage. This specification is intended to capture stressed funding conditions, under which rollover risk and liquidity premia may drive short-term borrowing costs above long-term rates, exacerbating liquidity stress exactly when the provider needs external funds most (Acharya et al., 2011; Wang et al., 2020).[4]

RA and RV refundable liabilities. Let $\Delta I_k^{\text{in}}(t)$ and $\Delta O_k^{\text{out}}(t)$ denote the aggregate refundable contribution inflows and repayment outflows for liability type $k \in \{\text{RA}, \text{RV}\}$. The respective liabilities evolve according to:

$$L^{\text{RA}}(t + \Delta t) = L^{\text{RA}}(t) + \Delta I_{\text{RA}}^{\text{in}}(t) - \Delta L_{\text{ret}}^{\text{RA}}(t) - \Delta O_{\text{RA}}^{\text{out}}(t), \tag{10}$$

$$L^{\text{RV}}(t + \Delta t) = L^{\text{RV}}(t) + \Delta I_{\text{RV}}^{\text{in}}(t) - \Delta L_{\text{ret}}^{\text{RV}}(t) - \Delta O_{\text{RV}}^{\text{out}}(t). \tag{11}$$

The retention terms, $\Delta L_{\text{ret}}^{\text{RA}}(t)$ and $\Delta L_{\text{ret}}^{\text{RV}}(t)$, capture how a resident's initial contribution differs from their final repayment. We specify these variables in Section 3.4 (see in particular Figure 3 and Appendix A).

3.4 Cash flow dynamics

This section details the cash flow components that enter the balance-sheet dynamics developed above.

Resident-flow dynamics. We begin by introducing a unified resident-flow framework for both the RA and RV segments. We design this framework to map facility-level resident dynamics into the model's principal cash flow components. In particular, changes in the resident census determine operating inflows and outflows, together with new refundable contributions. Moreover, because the repayment of refundable loans depends on individual length of stay (LOS), the framework also tracks the LOS composition of current residents. To capture these dynamics mathematically, we model the facility census as a continuous-time Markov chain (CTMC) bounded by maximum capacity (De Bruin et al., 2010). We introduce a regime shift at $t = 0$ triggered by an external shock, such as the COVID-19 pandemic. This allows us to simulate how both the size and demographic mix of the resident base dynamically adjust to severe stress conditions. Figures 2 and 3 summarise this framework, while Appendix A details the full continuous-time derivations.

Cash inflow. Over the interval $[t, t + \Delta t)$, the provider collects cash from four primary sources: (i) realised trade receivables, (ii) government subsidies, (iii) resident-funded payments including individual fees, RA loan inflow, and RV loan inflow, and (iv) other residual items.[5] We aggregate

[4] Emergency borrowing is assumed to arise solely from liquidity shortfalls relative to the applicable liquidity requirement; it is not used to finance CAPEX or other expenditures.

[5] These residual cash inflows, assumed constant, correspond to other predictable cash flows, explicitly excluding irregular windfalls such as one-off donations.

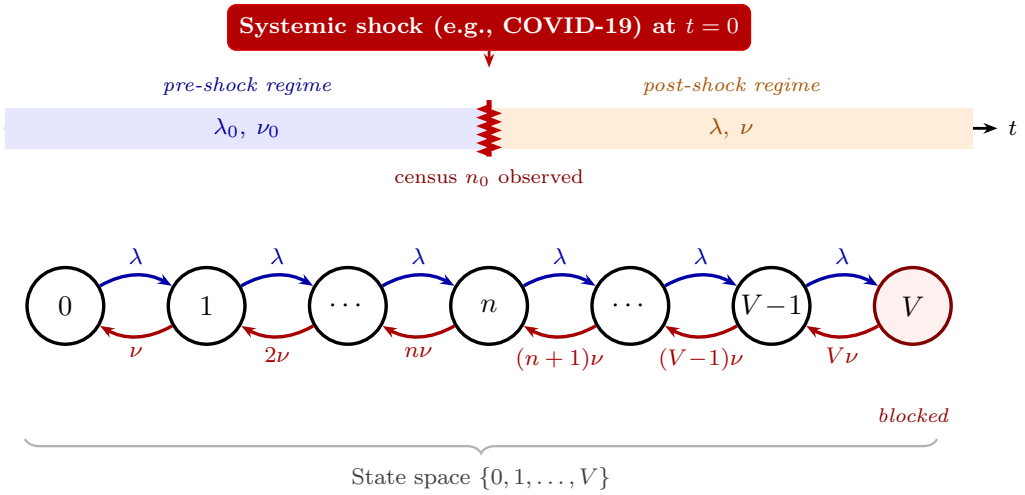

Figure 2. Resident flow framework and aggregate census dynamics for an aged care provider with maximum capacity V. At time $t = 0$, conditional on an observed initial census $n_0 = N(0)$, a systemic shock occurs. This shock triggers a regime shift: new arrivals and departures transition from their pre-shock baseline rates (λ_0, ν_0) to post-shock rates (λ, ν). A formal description of the model and the distribution of the post-shock census $N(t)$ are provided in Appendix A.

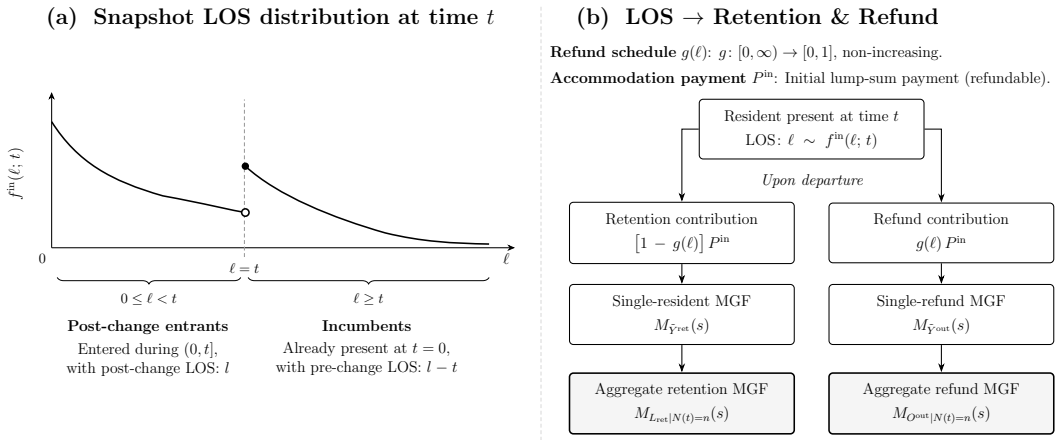

Figure 3. Length of stay (LOS)-based refund structure: snapshot LOS distribution (left panel) and LOS-dependent cash flow aggregation (right panel). The LOS distribution of residents, $f^{\text{in}}(\ell; t)$, together with the refund schedule $g(\ell)$ and incoming loan amount P^{in}, jointly determine the timing and magnitude of refundable outflows upon resident departure. Full details, including the moment generating function (MGF) expressions, are provided in Appendix A.

these inflows as:

$$\Delta I(t) = \underbrace{\Delta I^{\text{RTR}}(t)}_{\text{(i)}} + \underbrace{\Delta I^{\text{gov}}(t)}_{\text{(ii)}} + \underbrace{\Delta I^{\text{ind}}(t) + \Delta I^{\text{in}}_{\text{RA}}(t) + \Delta I^{\text{in}}_{\text{RV}}(t)}_{\text{(iii)}} + \underbrace{\Delta I^{\text{other}}(t)}_{\text{(iv)}},$$

Specifically, we model the individual components as follows:

- The provider recovers a constant rate γ of its outstanding trade receivables:

$$\Delta I^{\mathrm{RTR}}(t) = X^{r}(t) \cdot \gamma \cdot \Delta t. \tag{12}$$

- Government funding varies across providers. This variation occurs because means testing ties financial support directly to the socioeconomic profile of the resident base (Lyu et al., 2026). To maintain analytical tractability, the model holds this profile constant over the simulation horizon. Furthermore, we also assume the government locks in the nominal subsidy per resident (F^{gov}) for an entire year. Therefore, as inflation accumulates, the actual purchasing power of this subsidy steadily falls:

$$\Delta I^{\mathrm{gov}}(t) = N^{\mathrm{RACF}}(t) \cdot \frac{F^{\mathrm{gov}}}{\exp\left(\int_0^t \ln(1+\pi(s))ds\right)} \cdot (1-\psi_1) \cdot \Delta t, \tag{13}$$

  To track the fluctuating resident census in both the residential care ($N^{\mathrm{RACF}}(t)$) and retirement village ($N^{\mathrm{RV}}(t)$) segments, we employ the CTMC derived in Appendix A (and illustrated in Figures 2 and 3).

- Residents pay individual fees to cover daily expenses. Under the means-tested framework, these fees scale inversely with the government subsidies F^{gov}:

$$\Delta I^{\mathrm{ind}}(t) = \left[N^{\mathrm{RACF}}(t) \cdot (F^{\mathrm{RACF}} + \theta_{\mathrm{DA}} \cdot P_{\mathrm{DA}}) + N^{\mathrm{RV}}(t) \cdot F^{\mathrm{RV}}\right] \cdot (1-\psi_2) \cdot \Delta t, \tag{14}$$

  where F^{RACF} and F^{RV} denote the annual per-resident fee rates for RACF and RV residents. The term P_{DA} denotes the annual daily accommodation charge, and θ_{DA} denotes the proportion of RACF residents who fund accommodation through a daily payment.

- The RA and RV loan inflows capture the upfront, deposit-like funds the provider collects upon resident admission. We calculate these inflows as:

$$\Delta I^{\mathrm{in}}_{\mathrm{RA}}(t) = \Delta A^{\mathrm{RACF}}(t) \cdot \theta_{\mathrm{RA}} \cdot P^{\mathrm{in}}_{\mathrm{RA}}, \quad \Delta I^{\mathrm{in}}_{\mathrm{RV}}(t) = \Delta A^{\mathrm{RV}}(t) \cdot P^{\mathrm{in}}_{\mathrm{RV}}, \tag{15}$$

  where $\Delta A^{\mathrm{RACF}}(t)$ and $\Delta A^{\mathrm{RV}}(t)$ denote the number of new admissions over $[t, t+\Delta t)$, which are generated endogenously by the upward transitions of the resident-flow processes illustrated in Figure 2. Moreover, $P^{\mathrm{in}}_{\mathrm{RA}}$ and $P^{\mathrm{in}}_{\mathrm{RV}}$ are the RA and RV loan amounts received from newly admitted residents, respectively.[6] The term $\theta_{\mathrm{RA}} = 1-\theta_{\mathrm{DA}}$ is the proportion of newly admitted residents who fund the accommodation through a refundable deposit.

Cash outflow. Over $[t, t+\Delta t)$, the provider incurs cash outflows across three primary components: (i) operating expenditure (wages and other fixed expenditures), (ii) debt payments (interest and scheduled principal), and (iii) refunds for RA and RV liabilities triggered by resident departures. We

[6] While these deposit-like upfront loan amounts vary across providers, we model them as provider-specific homogeneous averages, thereby abstracting from idiosyncratic, resident-level contractual variations to maintain analytical tractability.

decompose these total outflows as:

$$\Delta O(t) = \underbrace{\Delta O^{\text{oprt}}(t)}_{\text{(i)}} + \underbrace{\Delta O^{\text{repay}}(t)}_{\text{(ii)}} + \underbrace{\Delta O^{\text{out}}_{\text{RA}}(t) + \Delta O^{\text{out}}_{\text{RV}}(t)}_{\text{(iii)}},$$

where:

- The operating expenses $\Delta O^{\text{oprt}}(t)$ comprise a base per resident operating cost O^{cost}, covering items such as food and basic medical supplies, and a residual fixed component O^{other}:

$$\Delta O^{\text{oprt}}(t) = \Big[(N^{\text{RACF}}(t) + N^{\text{RV}}(t)) \cdot O^{\text{cost}} \cdot (1+\varrho) + O^{\text{other}} \Big] \cdot \Delta t, \tag{16}$$

  where ϱ captures the policy-induced increase in per-resident wage costs associated with higher minimum required care hours.

- The provider services outstanding financial liabilities through both interest payments and scheduled principal amortisation:

$$\Delta O^{\text{repay}}(t) = \underbrace{\Big(L^s(t) + L^l(t)\Big)\left[\Big(1 + r^{\text{debt}}(t)\Big)^{\Delta t} - 1\right]}_{\text{Interest payment}} + \underbrace{\sum_{i\in\{s,l\}} \sum_{\ell=1}^{\min\{\ell^i_{\max},\, t/\Delta t\}} k^i(\ell)\, \Delta \tilde{L}^i_{\text{new}}(t - \ell\Delta t)}_{\text{Principal repayment}}. \tag{17}$$

  We assume that the principal is repaid through a linear schedule with kernel

$$k^i(\ell) = \begin{cases} 1/\ell^i_{\max}, & \ell = 1, \dots, \ell^i_{\max}; \\ 0, & \text{otherwise;} \end{cases}$$

  and $\Delta \tilde{L}^s_{\text{new}}(t)$ and $\Delta \tilde{L}^l_{\text{new}}(t)$ are the new borrowings:

$$\Delta \tilde{L}^s_{\text{new}}(t) = \Delta L^s_{\text{new}}(t) + L^s(0)\mathbb{I}_{\{t=0\}} \quad \text{and} \quad \Delta \tilde{L}^l_{\text{new}}(t) = L^l(0)\mathbb{I}_{\{t=0\}}.$$

  Here, to initialise this process, we treat the provider's debt balances at $t = 0$ as newly originated loans. With subsequent long-term borrowing prohibited ($t > 0$), new short-term debt functions strictly as emergency cash.

- Upon resident departures, the provider refunds the outstanding accommodation balances. We calculate these sudden liquidity outflows as:

$$\Delta O^{\text{out}}_{\text{RA}}(t) = \sum_{i \in \Delta D^{\text{RA}}(t)} P^{\text{out}}_{\text{RA},i}(t) \quad \text{and} \quad \Delta O^{\text{out}}_{\text{RV}}(t) = \sum_{i \in \Delta D^{\text{RV}}(t)} P^{\text{out}}_{\text{RV},i}(t). \tag{18}$$

  The continuous-time Markov chain detailed in Figure 2 endogenously generates the sets of departing residents, $\Delta D^{RA}(t)$ and $\Delta D^{RV}(t)$. Upon the departure of resident i, the provider repays the outstanding balance $P^{\text{out}}_{k,i}(t)$ associated with $k \in \{\text{RA}, \text{RV}\}$. This specific refund amount depends strictly on the resident's length of stay, which the framework tracks dynamically as

illustrated in Figure 3.

3.5 Liquidity management and prudential regulation

This section formalises the prudential regulatory environment, details the provider's stylised liquidity management rule, and establishes the metrics for evaluating liquidity risk.

3.5.1 Liquidity requirement under the dMLA

We first consider the liquidity requirement LR_t associated with the balance-sheet dynamics outlined in Equations (3) and (4). We assume each provider faces two distinct liquidity constraints.

1. *Liquidity crunch constraint*: At the end of each monthly period, liquid assets must remain non-negative;

2. *dMLA requirement*: Each quarter $t \in \mathcal{T}_M := \{3\Delta t, 6\Delta t, 9\Delta t, 12\Delta t\}$, the regulator requires the provider to hold liquid assets above the dMLA requirement.

We impose the following consolidated requirement:

$$\mathrm{LR}_t = \left(0.35 \sum_{j=t-3\Delta t}^{t-\Delta t} \left(\Delta O^{\mathrm{oprt}}(j) + r^{\mathrm{debt}}(j)(L^s(j) + L^l(j))\right) + 0.10\, L^{\mathrm{RA}}(t) + 0.02 L^{\mathrm{RV}}(t)\right) \cdot \mathbb{I}_{\{t\in\mathcal{T}_M\}}. \tag{19}$$

The dMLA term inside the brackets consists of three additive components at MLA inspection times: (i) 35% of cumulative core cash outflows over the preceding three months, proxied by operating outflows together with interest payments on outstanding short- and long-term borrowings; (ii) a buffer equal to 10% of RA liabilities; and (iii) a buffer equal to 2% of RV liabilities. The liquidity crunch constraint is imposed only on the remaining inspection periods.

3.5.2 Capital–liquidity tradeoff

When there is liquidity headroom, i.e. $X^l(t) - \mathrm{LR}_t > 0$, this surplus is employed as capital expenditure at rate κ (see Equations (3) and (4)).[7] Conversely, in case of a liquidity shortfall (that is, $X^l(t) - \mathrm{LR}_t < 0$), the provider undertakes emergency short-term borrowing (as from Equations (7) and (9)).

These dynamics give rise to a capital–liquidity tradeoff: reallocating surplus liquidity toward capital investment strengthens long-run capacity and resilience against the financial frictions of emergency borrowing, but reduces liquid buffers, potentially increasing short-run liquidity stress. This tradeoff motivates the need for an analysis of how the liquidity requirement constrains capital expenditure decisions.

[7] We assume that CAPEX is undertaken only at the quarterly inspection times, immediately following regulatory compliance verification. This specification mirrors realistic corporate treasury practices, where surplus cash is swept into long-term illiquid investments only after prudential buffers are secured.

3.5.3 Prudential metrics

To quantify the tradeoff described in Section 3.5.2, we measure the impact of the CAPEX investment rate κ on two event-based risk metrics: (i) the probability of a liquidity depletion (liquidity crunch) over the simulation horizon, and (ii) the probability of breaching the dMLA requirement.

We deliberately separate these metrics to distinguish true economic distress from mere regulatory non-compliance. This distinction allows us to demonstrate our central claim: breaching the static dMLA does not inevitably signal an actual liquidity crisis.

Let ω_j for $j \in \{1, 2, \ldots, \mathcal{N}\}$ denote a set of $\mathcal{N}$ independent simulated trajectories for a given provider.[8] For an event condition $\mathcal{E}$ monitored over a specific time set (such as the discrete time set $\mathcal{T}_M$), the empirical probability estimator $\hat{P}(\kappa)$ is given by $\hat{P}(\kappa) = \frac{1}{\mathcal{N}} \sum_{j=1}^{\mathcal{N}} \mathbb{I}_{\{\omega_j \in \mathcal{E}\}}$, where $\mathbb{I}_{\{\omega_j \in \mathcal{E}\}} = 1$ if the trajectory ω_j satisfies the conditions of event $\mathcal{E}$, and 0 otherwise. In words, $\hat{P}(\kappa)$ simply counts the fraction of simulated trajectories in which the event $\mathcal{E}$ occurs, providing a direct Monte Carlo estimate of its probability.

3.5.4 Why consider an alternative MLA?

Equation (19) imposes three rigid design choices that limit its cross-sectional applicability to heterogeneous providers during liquidity stress. Table 4 outlines these structural frictions and our proposed modifications. Accordingly, we introduce a forward-looking, risk-sensitive framework (rMLA), calibrated *ex ante* at the beginning of each year. Under the rMLA regime, Equation (19) becomes

$$\mathrm{LR}_t = \mathrm{rMLA} \cdot \mathbb{I}_{\{t \in \mathcal{T}_M\}}. \tag{20}$$

The empirically motivated construction and specification of the rMLA are presented in Section 5.4.

Table 4. Design constraints of the dMLA and proposed modifications.

dMLA design	Limitation	Friction	Modification
One-size-fits-all coefficients across providers	Fails to account for cross-sectional differences in balance-sheet capacity for liquidity risks.	Standardised rules ignore heterogeneous balance-sheet capacities and the rollover risks incurred during emergency borrowing (Acharya et al., 2011; Wang et al., 2020).	Provider-specific coefficients calibrated to asset-side characteristics.
Three-month lookback on financing outflows	Adjusts slowly to shifts in debt service: overstates required liquidity post-repayment and understates it post-borrowing.	Retrospective accounting metrics systematically mask underlying financial vulnerabilities during rapid market shifts (Jiang et al., 2024).	*Ex ante*, forward-looking calibration via multidimensional stress testing.
Proportional weights on RA and RV liabilities	Implicitly assumes refundable channels share proportional liquidity risk.	The RA and RV channels exhibit different turnover rates and stress sensitivities (Figure 5; Appendix A).	Channel-specific weights calibrated to empirical liquidity risk.

[8] Typically, $\mathcal{N}$ is set to 10^6.

4 Calibration and stress testing

This section sets out the calibration and stress-testing framework used in the study. It introduces the provider archetypes (Section 4.1), describes the baseline calibration of the dynamic model, and specifies the stress scenarios used to assess prudential performance.

4.1 Archetype provider

We identify six provider archetypes based on the sector's primary balance-sheet structures and funding mixes. Table 5 summarises the defining characteristics of each archetype, and Table 6 reports the balance-sheet and cash flow parameters (described in Sections 3.3 and 3.4, respectively) used in their calibration. These archetypes serve as transparent benchmark cases for stress-testing prudential outcomes under varying financial conditions.

Table 5. Provider archetypes used in the calibration.

Archetype	Description
RA Heavy	Provider with the highest share of RA liabilities, indicating the strongest reliance on refundable accommodation deposits as a funding source.
DA Heavy	Provider with the lowest share of RA liabilities, indicating the strongest reliance on daily accommodation payments.
Large CC	Large corporate-chain provider with the largest RACF resident base and a high level of internal trade receivables, treated as illiquid assets in the model.
RV Heavy	Provider with the largest retirement-village segment, measured by the share of residents in RV operations.
Small Regional	Small regional provider with the smallest RACF scale and a relatively high share of liquid assets, representing a more conservative balance-sheet structure.
Expn Heavy	Expansion-oriented provider with high long-term debt, a substantial capital base, and material exposure to the RV segment.

Notes: The six archetypes are designed to span the main balance-sheet structures and funding configurations observed in the sector rather than to match empirical population weights. Provider identities and absolute balance-sheet levels are anonymised.

4.2 Macroeconomic and financial calibration

Table 7 reports the baseline parameters we use to project the providers' balance-sheet dynamics. To ensure empirical validity, we calibrate these parameters using 2024 sector performance data, demographic benchmarks, and macroeconomic indicators.

Furthermore, we specify the refund schedule function, $g(\ell)$, introduced in Figure 3, for both RA and RV liabilities. The refundable balance declines with LOS through an annual retention charge of 2%, so that $g(\ell)$ is non-increasing in elapsed LOS. The retention period is capped at 5 years for RA balances and 15 years for RV balances, implying maximum cumulative retention rates of 10% and 30%, respectively.[9][10]

[9] For RACFs, the refund schedule function is imposed based on recent regulatory rules governing refundable accommodation deposits. In contrast, for RVs, where refund schedules are determined more flexibly and are not standardised by regulation, we specify a functional form calibrated to industry norms and chosen to maintain comparability across provider types.

[10] Although our simulation horizon is only 12 months, the facility is not empty at $t = 0$. As detailed in our resident-flow framework, we explicitly track the elapsed LOS distribution of incumbent residents who are already in the facility at the start of the simulation.

Table 6. Initial balance sheet and cash flow parameters for provider archetypes.

	RA Heavy	DA Heavy	Large CC	RV Heavy	Small Regional	Expn Heavy
General						
θ_{RA}	60.0%	20.0%	70.0%	39.5%	55.0%	49.0%
n^{RACF}	6,837	2,887	9,535	2,905	38	8,517
n^{RV}	—	580	—	1,957	—	3,555
L/X	101.263%	68.590%	99.274%	75.641%	55.280%	95.894%
Initial asset						
X^l/X	4.734%	6.042%	8.048%	5.932%	44.483%	7.695%
X^c/X	94.329%	92.464%	91.361%	91.445%	54.793%	91.479%
X^r/X	0.936%	1.494%	0.591%	2.622%	0.723%	0.826%
Initial liability						
L^{RA}/L	86.148%	55.198%	63.593%	40.540%	81.116%	47.496%
L^{RV}/L	—	20.944%	—	32.576%	—	17.530%
L^s/L	13.392%	20.190%	13.691%	12.841%	12.097%	11.682%
L^l/L	0.459%	3.668%	22.715%	14.043%	6.787%	23.293%
Cash flow (AUD in thousands)						
$P^{\text{in}}_{\text{RA}}$	366.163	722.391	477.334	537.437	284.682	457.038
P_{DA}	28.011	55.263	36.516	41.114	21.778	34.963
$P^{\text{in}}_{\text{RV}}$	—	389.166	—	343.948	—	268.953
F^{gov}	108.782	135.337	134.587	152.122	115.592	132.210
F^{RV}	—	7.920	—	7.000	—	5.474
F^{RACF}	27.127	25.413	25.717	24.912	26.483	25.842
I^{other}	11,626	19,694	70,018	33,433	57	74,700
Expense (AUD in thousands)						
O^{cost}	128.177	119.480	142.964	93.384	99.763	93.508
O^{other}	178,574	112,252	211,318	71,234	1,204	105,900

Notes: Each column represents a distinct provider archetype, labelled by its defining balance-sheet or revenue feature. We calibrate the parameters for each representative provider using their published 2024 financial statements. In the notation, θ_{RA} denotes the proportion of RACF residents funding their accommodation via refundable deposits, while n^{RACF} and n^{RV} denote the total resident census in the RACF and RV facilities, respectively. Consistent with our macroeconomic framework (Section 3.2), we express all monetary parameters in real terms, holding their inflation-adjusted values constant over the simulation horizon (in Australian dollars). Finally, to guarantee internal model consistency, we calibrate rather than directly observe several key metrics, detailing this procedure in Appendix B.1.

Table 7. Baseline macroeconomic and financial parameters.

Parameter	Explanation	Value	Remark
T	Total periods (months)	12	12-month simulation
ν_0^{RACF}	Departure rate when $t < 0$: RACF (yr^{-1})	0.3	StewartBrown (2025a)
ω^{RACF}	Initial occupancy: RACF (%)	95	
ν_0^{RV}	Departure rate when $t < 0$: RV (yr^{-1})	0.1	StewartBrown (2025b)
ω^{RV}	Initial occupancy: RV (%)	88	
δ_1	Contractual spread (%)	1	RBA (2026)
δ_2	Term spread (%)	3	RBA (2026)
ϱ	Increase in operating cost per resident (%)	7.5	StewartBrown (2025a)
μ_0	Payment rate (yr^{-1})	24	Fortnightly payment
$\tilde{\psi}$	Rising resident contribution (%)	4	Wells (2024)
ψ_1	Rising receivables: >1 mon (%)	0.5	Remark 3.1
ψ_2	Resident receivables: >1 mon (%)	13.5	Remark 3.2
γ	Receivable realisation rate (yr^{-1})	10.4	Remark 3.2
ϕ_1	Short-term funding intercept	-0.23	DHDA (2024)
ϕ_2	Leverage loading	0.33	
$l^s_{\max}$	Short-term repayment (months)	7	RBA (2026)
$l^l_{\max}$	Long-term repayment (months)	60	

Notes: Macroeconomic and financial variables, including the contractual spread (δ_1), term spread (δ_2), and the repayment horizons, are calibrated using historical cash rate targets and yield curve data sourced directly from the Reserve Bank of Australia (RBA) Statistical Database (RBA, 2026) for the period of September 2018 to January 2026. The short-term funding parameters (ϕ_1 and ϕ_2) are calibrated based on an average liability-to-asset ratio of 70%. This reflects the assumption that under the baseline calibration, a liability-to-asset ratio of 70% represents the threshold where short-term and long-term financing costs reach parity, preventing term-structure inversion.

4.3 Stress-testing framework

To evaluate the providers' prudential resilience, we design a stress-testing framework that contrasts a baseline environment with a severe shock scenario. We calibrate this shock to the extreme conditions observed during the late-pandemic period (2021–2022). Four dimensions are considered: (i) the inflation path, $\pi(t)$, generated by the VAR model; (ii) resident-flow dynamics, captured by the admission intensity, λ, and the per-resident departure rate, ν; (iii) the yield spread on short-term liquid investments; and (iv) the term structure of borrowing costs, reflecting the spread between short- and long-term debt rates.

The parameter choices for both scenarios are reported in Table 8. In the first two dimensions, the shock scenario reflects an ACQSC-proposed shock involving a 1.3% increase in inflation and a 7.7% decline in occupancy. The final two dimensions are incorporated to assess whether additional factors may also materially influence the results. Further discussion of the rationale for selecting these four dimensions is provided in Appendix B.2. Sensitivity analysis for the stress-scenario calibration is reported in Appendix B.3. The analysis indicates that occupancy-related shocks are the dominant driver, followed by inflation, while the remaining two dimensions appear to have only a limited effect on the results in the present setting.

Table 8. Stress-test design: shocks to resident census, economic, and financial conditions at $t = 0$.

Scenario	$\Delta\pi(0)$	λ	ν	$\Delta\delta_1$	$\Delta\phi_1$	$\Delta\phi_2$
Baseline	0	λ_0	ν_0	0	0	0
Shock	1.3%	$0.85\lambda_0$	$1.15\,\nu_0$	−0.5%	0.125	0.025

Notes: The inflation shock is implemented as a structural shift applied to the initial VAR-generated trajectory. Figure 4 presents the implied paths of inflation and the nominal interest rate under the baseline and ACQSC-shock scenarios. We set $p = 2$ in the calibration; full estimation details are provided in Appendix B.2. The expected occupancy ratio after one year is approximated via Remark A.2 in Appendix A. The parameter $\Delta\delta_1$ denotes the compression of money-market premia under stress. $\Delta\phi_1$ and $\Delta\phi_2$ adjust the short-term funding-cost parameters in Equation (9) to reflect a lower term-structure inversion threshold.

Figure 4 traces the implied macroeconomic paths, with the shock calibrated to a 1.3 percentage-point average increase in inflation over one year (approximately three standard deviations relative to the baseline forecast). Figure 5 illustrates the joint effects of resident-flow and macroeconomic shocks for the RV Heavy provider, with the resident-flow channel shown in Panel 5(a) and the combined effect on refund cash flows in Panel 5(b). The resident census declines in both RACF and RV as admissions fall and departures rise, with a weaker effect in RV owing to its lower turnover (Panel 5(a)). This attenuation does not carry over to retention deductions: the shock accelerates the exit of residents with relatively large accrued retention amounts, leaving RV retention comparatively higher than in RACF (Panel 5(b)). Across both settings, the shock effect is front-loaded, mirroring the macroeconomic pattern in Figure 4, and most pronounced in RACF, where departures and refund outflows rise sharply in early periods before gradually attenuating.

5 Results

This section presents the numerical findings of our stochastic simulation framework. Initial observations reveal a concerning dynamic: the dMLA requirement distorts the capital–liquidity tradeoff

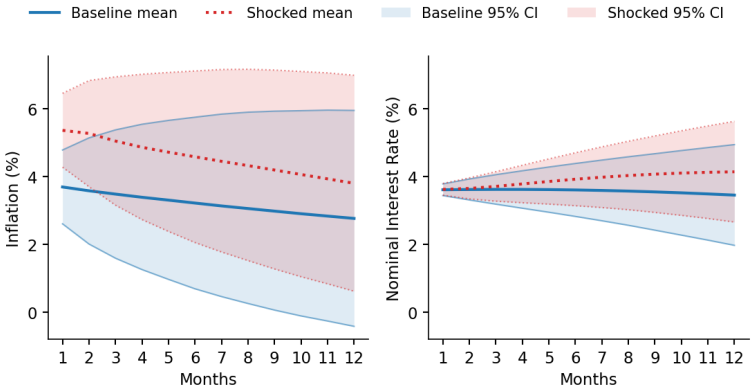

Figure 4. Simulated macroeconomic paths under baseline and shock scenarios. The figure plots the conditional forecast of inflation and the nominal interest rate from the estimated VAR(2), comparing the baseline trajectory with a scenario featuring a one-off structural inflation shock between 0 and Δt (calibrated to a 1.3 p.p. average increase over a year, approximately three standard deviations).

in highly heterogeneous ways across provider archetypes. Through a deeper analysis of these distortions, we propose a risk-sensitive alternative, the rMLA, which expands the feasible investment frontier under baseline conditions for the majority of archetypes while preserving resilience under stress.

5.1 dMLA compliance across archetypes

Intuitively, when providers employ a larger share κ of the cash surplus as CAPEX, they lower their liquid buffers and increase the likelihood of needing emergency borrowing. An expected capital–liquidity tradeoff emerges: higher κ should drive up the probability of a liquidity requirement breach, particularly under the exogenous shocks detailed in Table 8. However, our simulations reveal that the dMLA distorts this tradeoff (Figure 6), potentially penalising distinct business models asymmetrically.

Our simulation shows that providers heavily reliant on the RA channel (the RA Heavy and Large CC archetypes) exhibit a greater propensity for dMLA breaches. Under severe stress, the RA Heavy provider breaches the dMLA with over 80% probability, and the Large CC with certainty, irrespective of κ. Even under baseline conditions, the Large CC breaches the dMLA once κ exceeds 0.5. This pattern appears to be driven by dMLA imposing a high 10% statutory weight on RA liabilities, which translates to a larger liquidity buffer requirement. As a result, these institutions become disproportionately vulnerable, struggling to maintain dMLA compliance under exogenous shocks. Consequently, these findings highlight the need to evaluate whether dMLA imposes an outsized regulatory burden on these two business models.

By contrast, the Small Regional provider demonstrates a distinct pattern. Despite its similar reliance on the RA channel, it exhibits a lower dMLA breach probability than the RA Heavy and Large CC archetypes. Specifically, under the exogenous shock, the Small Regional provider maintains a zero breach probability for κ up to 0.7, and even at the maximum CAPEX investment rate ($\kappa = 1$), the probability remains below 20%. This resilience stems from the Small Regional provider endogenously maintaining proportionally larger *ex ante* liquidity buffers. Consequently, it remains insulated from regulatory breaches within our simulations. These findings suggest that for smaller

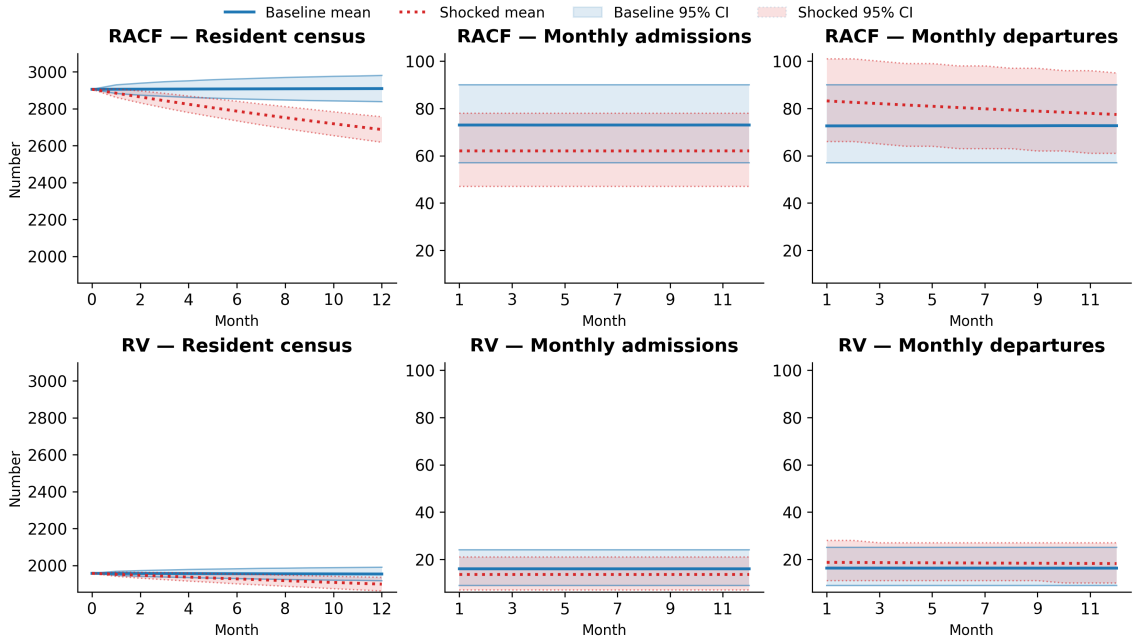

(a) Resident census, admissions, and departures.

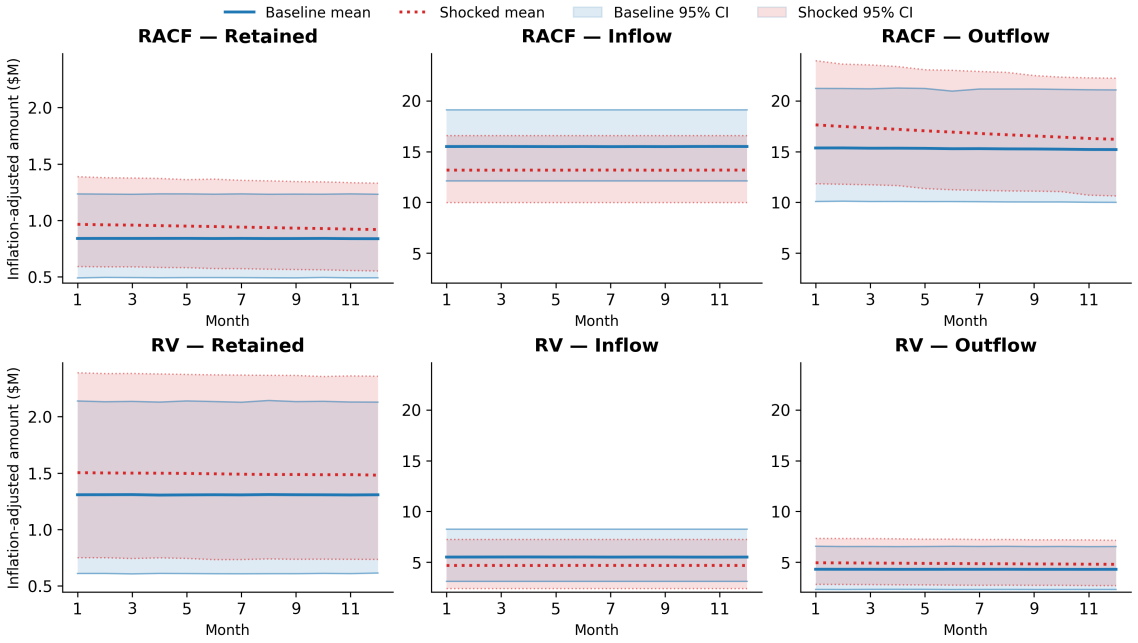

(b) Retained refunds and refund inflows/outflows.

Figure 5. Simulated RACF and RV census dynamics and refund-related cash flow components for the RV Heavy provider, under the baseline (blue) and shock (red) scenarios. Panel (a) reflects resident-flow dynamics alone, while Panel (b) additionally incorporates the macroeconomic shock.

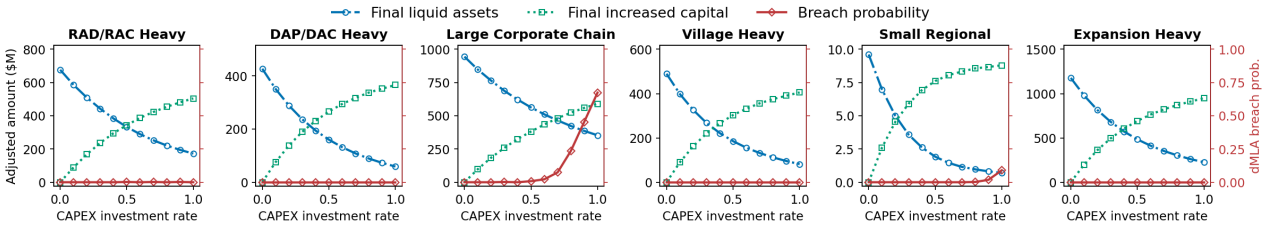

(a) Baseline.

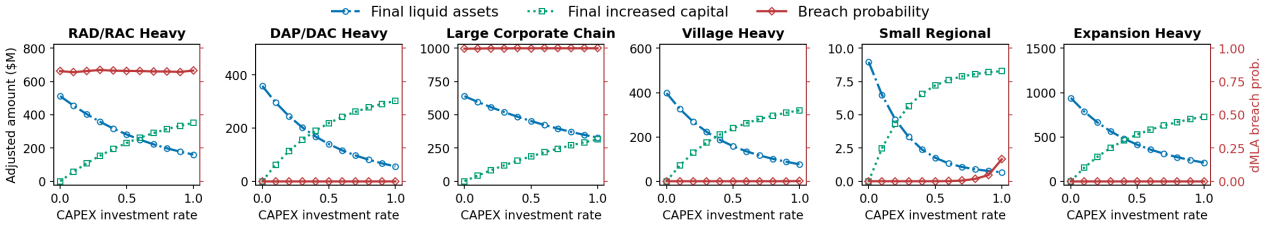

(b) Shock.

Figure 6. Liquid assets (blue), capital increase (green) and probability of breaching the dMLA (red) by rate of capital expenditure under the baseline (top) and the shock (bottom) scenario.

institutions, the dMLA may lack sufficient binding force: their internal liquidity targets, calibrated to self-assessed risk, already exceed the statutory requirement.

Finally, our simulations show that the regulatory compliance of the DA Heavy, RV Heavy, and Expn Heavy archetypes is less sensitive to changes in κ compared to providers heavily reliant on the RA channel. From a prudential perspective, the dMLA framework applies a statutory weight of merely 2% to RV liabilities, compared to 10% for RA liabilities. Assuming comparable overall profitability across RACF and RV segments, the more heavily a provider relies on the RV segment, the smaller the relative impact of the liquidity buffer requirement. From a risk perspective, as illustrated in Figure 5, the RV segment remains more stable than the RACF segment under exogenous shocks, resulting in lower liquidity risk.

5.2 Unpacking the drivers of dMLA breaches

Our annual projections reveal that the dMLA distorts the capital–liquidity tradeoff. However, this annualised perspective fails to capture the precise timing of dMLA breaches. To further explore the underlying drivers of dMLA breaches, we examine how the breaches occur across the quarterly inspection times. Given that archetypes with an RV segment exhibit only limited stress (Section 5.1), we restrict the analysis to those operating exclusively in the RACF segment under both baseline and shock scenarios.

For the RA Heavy and Large CC archetypes, our simulations reveal that dMLA breaches are concentrated in the first two quarters (Figure 7). This pattern suggests that early breaches are driven by near-term financing pressure rather than by persistent liquidity weakness over the year. Specifically, because we assume providers amortise emergency short-term liabilities over seven months (Table 7), they face severe repayment pressure early in the year. Figure 8 further confirms that breach risk is sensitive to the assumed short-term repayment horizon. Under the shock scenario, this early-quarter vulnerability becomes even more pronounced, while breach probabilities remain zero in Q3 and Q4. Taken together, these results suggest that early dMLA breaches for these two archetypes

are largely driven by the backward-looking treatment of financing outflows in the dMLA design.

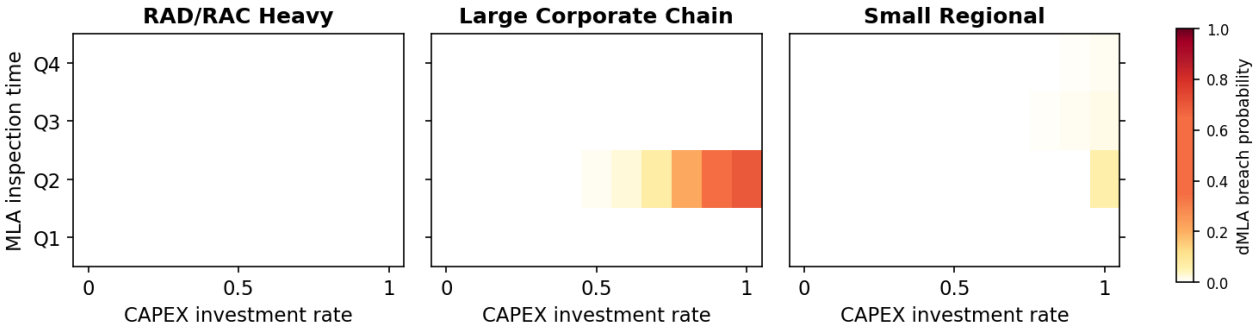

(a) Baseline.

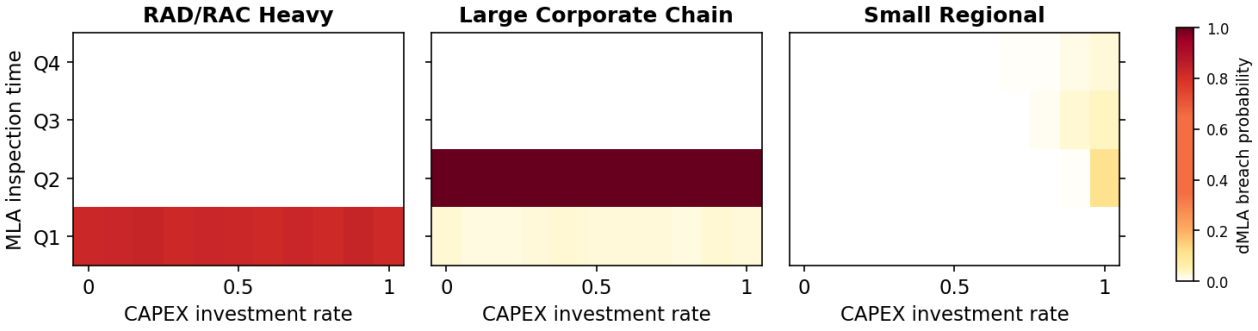

(b) Shock.

Figure 7. Probability of breaching the dMLA at quarterly inspection time across RACF-only provider archetypes under the baseline and shock scenarios.

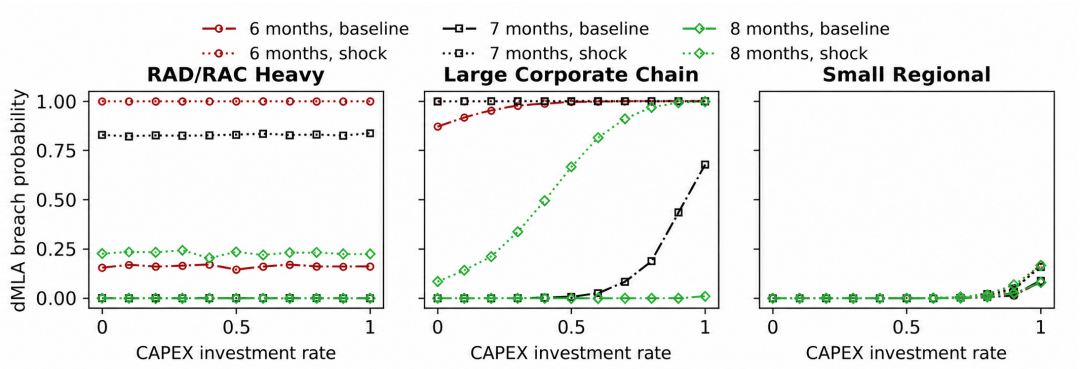

Figure 8. Sensitivity of dMLA breach probabilities to alternative short-term debt repayment horizons across RACF-only provider archetypes. A shorter short-term repayment horizon represents tighter refinancing conditions and greater near-term liquidity stress, whereas a longer horizon reflects more gradual amortisation and a smoother cash flow adjustment path.

By contrast, for the Small Regional provider, the relatively high share of liquid assets delays the onset of dMLA breaches. Although the simulated breach probability also declines after Q2, the decline is less pronounced than for the other two archetypes.[11] This distinction implies that, for smaller providers, the dMLA signals underlying liquidity distress to some extent, rather than mere timing mismatches in regulatory accounting.

[11] This decline is mainly driven by the attenuation of the shock over the year, as illustrated in Figures 4 and 5.

5.3 dMLA breach versus liquidity crunch

The preceding results indicate that breaching the dMLA does not necessarily coincide with a genuine liquidity event, and that satisfying the dMLA does not, on its own, ensure that a provider can withstand stress. To separate regulatory compliance from underlying liquidity risk, we next compare the dMLA breach probability with the probability of a liquidity crunch (Section 3.5) across providers and scenarios.

To facilitate this comparison, we reparameterise the analysis in terms of an initial buffer rate, $B \in [0, 1]$, defined as the share of liquid assets that the provider retains as a liquidity reserve at $t = 0$:

$$B \equiv \frac{\text{Retained initial buffer amount}}{X^l(0)}. \tag{21}$$

The complementary amount $(1-B)X^l(0)$ is immediately allocated to capital expenditure. To isolate the role of the initial buffer and avoid understating liquidity risk through endogenous buffer rebuilding, we further assume that all subsequent surplus liquidity is converted into capital, $\kappa = 100\%$ for all $t > 0$.

Figure 9 maps this buffer rate B against the probability of a liquidity crunch, offering a reinterpretation of the dMLA breach patterns in Figure 6. Specifically, the RA Heavy archetype exhibits minimal vulnerability even at a zero buffer rate. Similarly, while the Large CC provider faces moderate risk, it circumvents the liquidity risk using only a minimal buffer. These findings demonstrate that for certain large providers dependent on the RA channel, a dMLA breach does not imply genuine liquidity stress. This regulatory disconnect suggests that their operational scale provides an inherent capacity to absorb shocks, making them far more resilient than the dMLA framework implies.

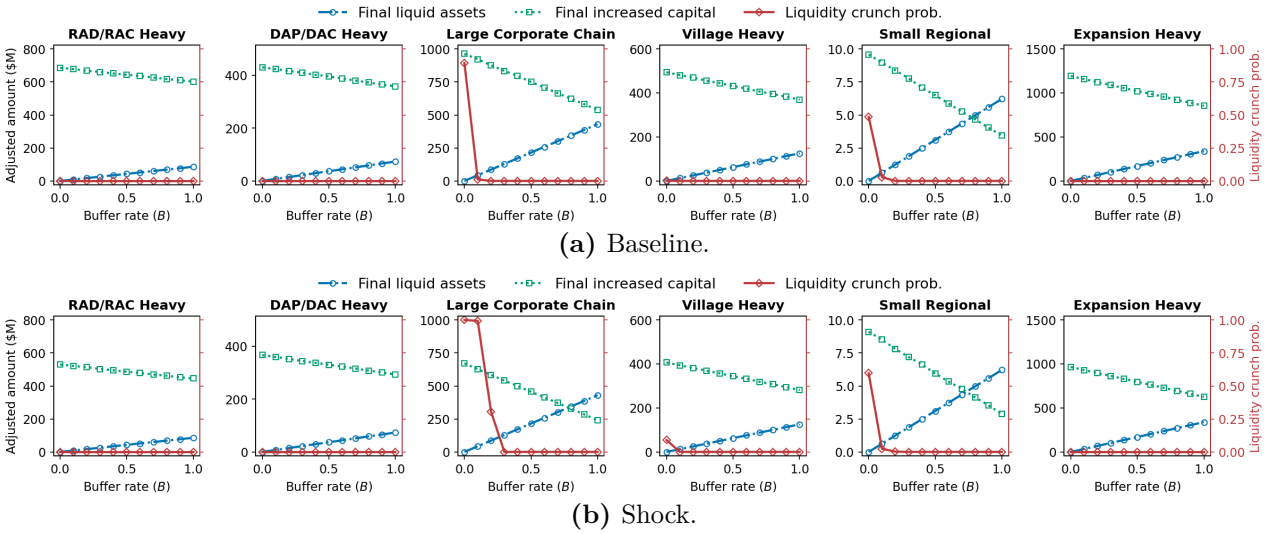

(a) Baseline.

(b) Shock.

Figure 9. Simulated liquidity crunch probability as a function of the buffer rate (B) across provider archetypes.

For the Small Regional archetype, the dMLA-breach curve with respect to κ in Figure 6 mirrors the profile of the liquidity crunch curve with respect to the buffer rate, B. This suggests that, compared to the RA Heavy and Large CC archetypes, the dMLA is more closely aligned with

underlying liquidity risk for this specific provider. Nevertheless, at a zero buffer rate, the crunch probability exceeds the likelihood of a dMLA breach, indicating that the dMLA understates the true extent of liquidity risk by ignoring balance-sheet capacity, consistent with our conjecture in Section 5.1.

5.4 Proposed rMLA specification

The preceding analysis highlights limitations of the dMLA. By relying heavily on backward-looking accounting metrics, this one-size-fits-all requirement does not fully capture the randomness of resident flows and macroeconomic shocks. Furthermore, it overlooks providers' heterogeneous capacities to absorb liquidity stress.

To address these shortcomings, we propose the rMLA: a risk-sensitive, rule-based liquidity requirement. We derive the rMLA by simulating the minimum buffer that a population of synthetic providers need to survive under shock (Table 8). Projecting this required buffer onto a parsimonious set of a provider's initial financial features yields the linear rMLA formula.

5.4.1 Sample construction and variables

We generate a sample of 5,000 synthetic providers. The sample extends well beyond the six archetypes considered earlier, while accounting constraints preserve its realism. To capture plausible yet more concentrated structures relevant for tail-risk stress testing, we additionally permit limited extrapolation beyond the archetype space. The approach expands the coverage of provider characteristics without generating implausible outliers. See Appendix C.1 for additional details.

We seek to quantify the precise prudential liquidity that a provider requires to survive an extreme exogenous shock under the most aggressive feasible capital deployment ($\kappa = 1$). We formalise this through $B^\star$, defined as the smallest value of B (Equation (21)) such that the probability of a liquidity crunch remains below 1% under the severe shock scenario, conditional on $\kappa = 1$.[12] Formally, let $\xi_j^* \in \mathbb{R}^{24}$ denote the vector of initial features ($t = 0$) for the j-th synthetic provider, comprising the inputs required by the simulation framework (Section 3).[13] Over the one-year horizon, we computationally derive the minimum buffer rate for the j-th synthetic provider, denoted as $B_j^\star = f(\xi_j^*)$.

To derive an interpretable prudential rule that facilitates comparison with the dMLA, we select a parsimonious subset of explanatory variables from ξ_j^*. We begin with all asset, liability, and cash flow variables of the synthetic providers and then trim this set to mitigate multicollinearity. Underlying cash flow dynamics are proxied by capital assets and trade receivables, and debt-servicing costs by outstanding financial liabilities. RA liabilities are retained for consistency with the dMLA framework, whereas RV liabilities are dropped because they correlate strongly with other preserved variables. Ultimately, this dimension reduction yields a parsimonious set of five variables: capital assets ($X^c(0)$),

[12] Sensitivity analysis across alternative liquidity crunch thresholds (from 0.5% to 1.5%) shows that the resulting rMLA parameters shift by less than 2.7%, leaving our main conclusions unchanged.

[13] The 24 provider-specific parameters subject to interpolation are: n^{RACF}, n^{RV}, V^{RACF}, V^{RV}, λ^{RACF}, λ^{RV}, θ_{RA}, $P_{\text{RA}}^{\text{in}}$, P_{DA}, $P_{\text{RV}}^{\text{in}}$, F^{gov}, F^{RACF}, F^{RV}, O^{cost}, O^{other}, I^{other}, $X^l(0)$, $X^c(0)$, $X^r(0)$, $L^{\text{RA}}(0)$, $L^{\text{RV}}(0)$, $L^s(0)$, $L^l(0)$, and κ. All remaining parameters are held constant across providers.

trade receivables ($X^r(0)$), short-term liabilities ($L^s(0)$), long-term liabilities ($L^l(0)$), and RA liabilities ($L^{\text{RA}}(0)$).

For the j-th provider, we model the required minimum buffer rate, $B_j^\star$, as a linear function of this parsimonious subset of variables. To maintain consistency with $B_j^\star$, which is scaled by initial liquid assets ($X^l(0)$), the five explanatory variables are expressed as ratios to the same base.[14] Because the rMLA is an *ex ante* calibration, all covariates capture initial balance-sheet states at $t = 0$; for notational brevity, we suppress the time index hereafter. Standardising these ratio components yields our final empirical specification:

$$B_j^\star = \beta_0 + \beta_1 \widetilde{X^c/X^l}_j + \beta_2 \widetilde{X^r/X^l}_j + \beta_3 \widetilde{L^s/X^l}_j + \beta_4 \widetilde{L^l/X^l}_j + \beta_5 \widetilde{L^{\text{RA}}/X^l}_j, \tag{22}$$

where the tilde indicates that the covariate has been standardised. The coefficient vector $\boldsymbol{\beta} = (\beta_0, \beta_1, \ldots, \beta_5)$ is estimated using ridge regression (Hastie et al., 2001).

5.4.2 Estimated rMLA rule

The rMLA is obtained by first reversing the transformation of the explanatory variables and modifying the value of the regression coefficients accordingly (see Appendix C.2 for full details). For a given provider, this yields the following relationship:

$$\widehat{\text{rMLA}} = \Bigg(\underbrace{0.358X^l - 0.343X^c + 4.072X^r}_{\substack{\text{Balance-sheet adjustment} \\ \text{for asset composition}}} + \underbrace{1.419\,L^s + 0.246\,L^l}_{\substack{\text{Funding pressure implied by} \\ \text{short- and long-term debt}}} + \underbrace{0.082\,L^{\text{RA}}}_{\substack{\text{RA liability} \\ \text{component}}} \Bigg)^+. \tag{23}$$

Several analytical insights follow from this setup. The asset side block serves as a proxy for balance-sheet strength. For instance, a larger liquid asset base (X^l) proxies for operating scale, thereby increasing the required absolute buffer. Conversely, a stronger capital base (X^c) reduces the required buffer, because it equips the provider with greater collateral capacity to raise emergency borrowings. By contrast, the positive coefficient on receivables (X^r) penalises assets that lack cash immediacy.[15] Finally, the liability coefficients (L^s, L^l, and L^{RA}) precisely capture the debt-servicing burdens and event-driven cash drains imposed by different funding sources.

Figure 10 plots the simulated minimum buffer rate, $B^\star$, against the unconstrained predicted buffer rate (i.e., the linear combination in Equation (23) prior to applying the non-negativity floor). We deliberately plot the pre-truncation values to display the unrestricted goodness-of-fit of the raw linear projection across the entire sample space. To facilitate cross-sectional comparison, both metrics are normalised by initial liquid assets rather than expressed in absolute dollar amounts. As the

[14] We adopt a ratio specification rather than an absolute-level model for three reasons. First, it eliminates size-driven bias: estimating liquidity buffer levels (i.e., $B_j^\star X^l(0)$) introduces an intercept that systematically overstates the requirements for smaller providers in our simulation. Second, it preserves parsimony; achieving equivalent economic interpretation in an absolute framework would require an additional covariate. Finally, it ensures institutional comparability: the ratio specification admits a non-intercept form post-transformation, aligning structurally with the dMLA formula.

[15] Although the coefficient on X^r appears large in absolute terms, its standardised value is comparable to the other regressors (Appendix C.2). This magnitude simply reflects the low absolute level of receivables compared to other balance-sheet items.

figure illustrates, the predicted values cluster tightly along the 45-degree line, indicating that our parsimonious linear formula captures the complex, non-linear liquidity dynamics generated by the simulation.

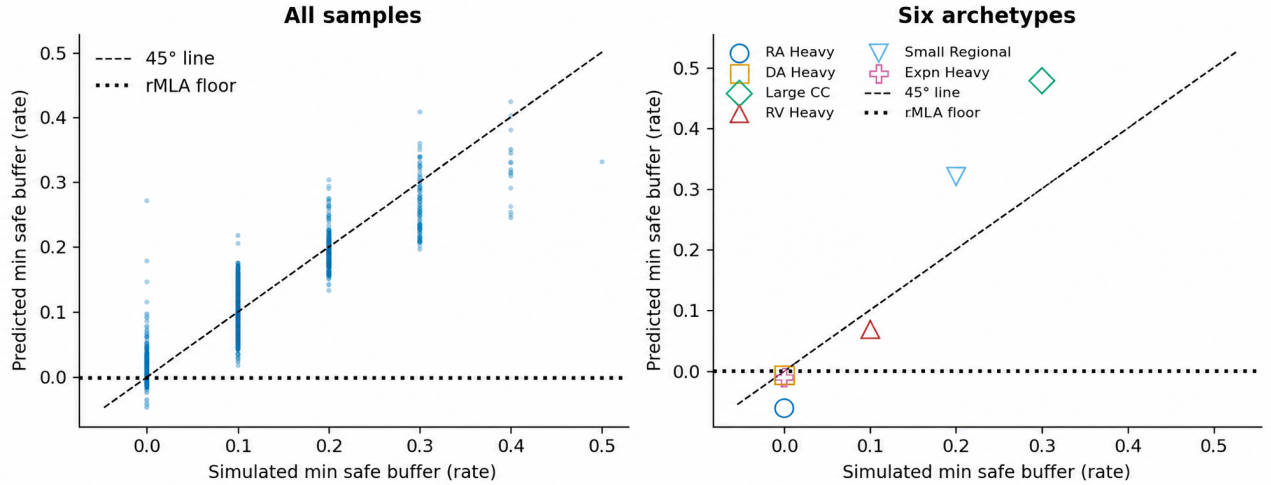

Figure 10. Simulated versus predicted minimum liquidity buffer rates for all synthetic providers (left panel) and the archetypes (right panel). The 45-degree line denotes perfect agreement. Note that the predicted values are plotted pre-truncation (i.e., before applying the zero floor) to illustrate the unconstrained linear fit.

5.4.3 Comparison with the dMLA

Relative to the dMLA, the rMLA provides a more risk-sensitive measure of liquidity need:

- **Recognising asset-side capacity.** The dMLA is driven primarily by liability- and outflow-based proxies, whereas the rMLA additionally incorporates asset-side characteristics that reflect a provider's overall balance-sheet capacity. This distinction is conceptually relevant since the access to liquidity depends not only on obligations coming due, but also on the collateral value of the asset base (Donaldson et al., 2020). This interpretation is further corroborated by the robustness tests for the rMLA coefficients concerning the short-term borrowing repayment horizon (Appendix C.3): a condensed repayment horizon imposes a heavier liquidity burden, thereby yielding a higher rMLA coefficient associated with assets.

- **Forward-looking vs. backward-looking.** The financing-expense component of the dMLA is anchored in backward-looking realised accounting positions, capturing only historical interest expenses rather than future repayment obligations. This structural lag is highly problematic in a prudential context, as such metrics adjust too slowly to sudden shifts in underlying refinancing conditions. Consistent with this concern, Jiang et al. (2024) demonstrate that static book values systematically mask mark-to-market losses during aggregate shocks, diverging substantially from market valuations. Consequently, anchoring regulatory buffers to retrospective accounting data can severely underestimate true liquidity needs. By contrast, the *ex ante* design of the rMLA proactively incorporates the burden of both principal and interest repayments over

the relevant stress horizon, rather than proxying financing pressure through historical interest expenses alone.

- **Downweighting refundable liabilities.** A divergence between the rMLA and the dMLA emerges in the treatment of the two refundable funding channels. While the rMLA retains a reduced weight for RA liabilities, the coefficient for RV liabilities is driven entirely to zero. This setup aligns with Figure 5, which demonstrates that the RV segment is less risky under stress. Rather than acting as a rapid liquidity drain under shocks, the RV segment functions as a stabiliser relative to the RACF segment. This resilience justifies eliminating the RV penalty within the prudential framework, ensuring that regulation does not inefficiently constrain capital capacity by penalising more stable funding sources.

5.5 Balance sheet implications

We now evaluate how the dMLA and rMLA reshape providers' balance sheets. By directly comparing these two requirements across various stress scenarios, we demonstrate the efficiency of our proposed framework.

5.5.1 Overview of the capital–liquidity tradeoff

To illustrate the capital–liquidity tradeoff, Figure 11 plots the present value of changes in capital assets against the present value of changes in liquid assets. Each marked point on these frontiers represents a specific investment rate ($\kappa \in \{0, 0.25, 0.5, 0.75, 1\}$), with κ increasing from the bottom-right to the top-left. This allows for a direct comparison of the dMLA and rMLA constraints across both baseline and shock scenarios.

As illustrated in the figure, for most archetypes, the rMLA extends the frontier relative to the dMLA, particularly under baseline conditions. Specifically, the frontier elongates toward the top-left, reaching into the region characterised by lower liquidity and higher capital assets. This extension shows that risk-sensitive regulation materially broadens a firm's feasible investment choices. Our findings in the aged care sector are thus consistent with Kara and Ozsoy (2020)'s theoretical predictions and corroborate Roberts et al. (2023)'s empirical evidence from the banking industry.

Furthermore, our simulations indicate that systemic stress compresses these frontiers toward the origin. While the initial liquidity drain in the aged care sector is driven by exogenous events rather than strategic depositor behaviour, the resulting contraction illustrates how binding liquidity constraints amplify exogenous shocks through an endogenous funding-cost feedback loop. Specifically, emergency borrowing under stress raises subsequent debt-servicing costs, which in turn tightens the feasible capital–liquidity set. Despite originating from a different fundamental friction, this funding-cost amplification conceptually mirrors the liquidity spirals and fire-sale frictions established in the banking literature (see, e.g., Vives 2014).

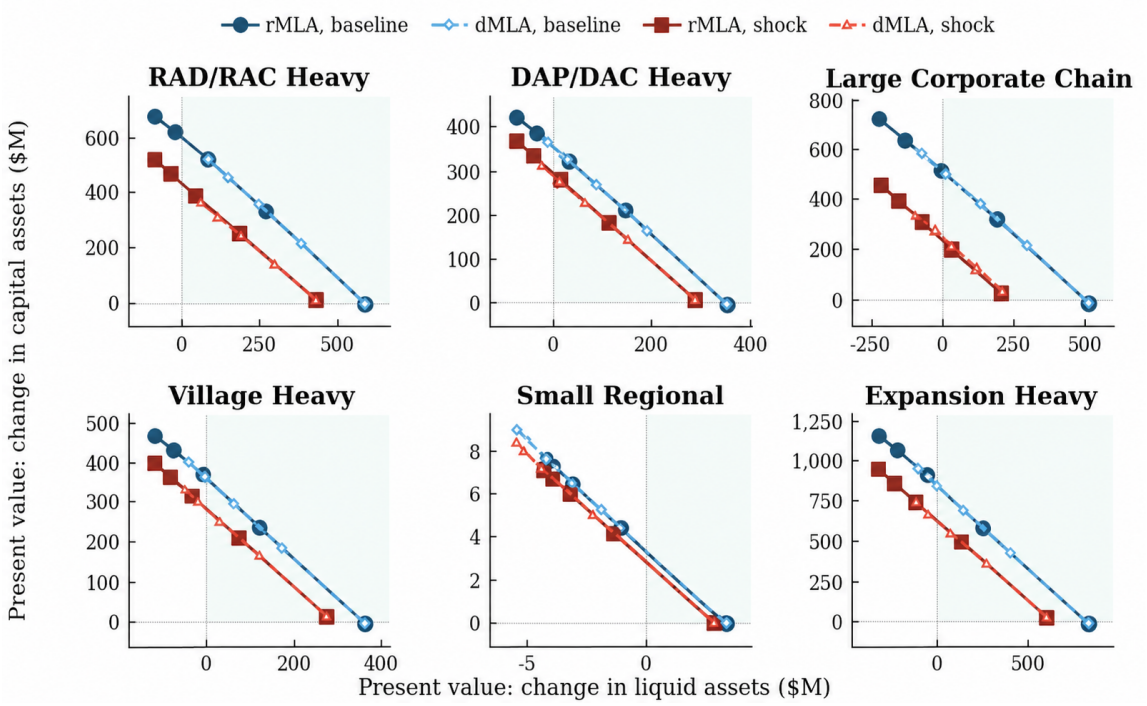

Figure 11. Capital–liquidity frontiers under the dMLA and the proposed rMLA. Each panel traces the feasible combinations of discounted liquidity change and discounted capital accumulation as the CAPEX investment rate, κ, varies over $\{0, 0.25, 0.5, 0.75, 1\}$, with κ increasing from the bottom-right to the top-left.

5.5.2 rMLA expands capacity for capital investment

To quantify this capital–liquidity tradeoff, Table 9 reports the present value of incremental capital investment under both requirements. Under the baseline scenario, for most provider archetypes and CAPEX rates κ, the proposed rMLA frees additional resources compared to the dMLA. By relaxing rigid regulatory constraints, the rMLA enables providers to deploy these resources into potentially higher-return capital expenditure. The magnitude of these additional resources varies across archetypes and is explained by the negative coefficient on the capital base (X^c) in Equation (23). Providers with larger capital stocks face a lower rMLA, freeing up liquidity that can be redeployed into capital assets. The Small Regional provider remains the sole exception: in this case, under the dMLA, this archetype has a higher capital expenditure capacity.

These baseline results highlight a distortion in the existing framework. By ignoring asset-side strength, the dMLA forces well-capitalised providers to hoard cash while under-protecting smaller entities (such as the Small Regional archetype) against idiosyncratic risks. Conversely, the rMLA incorporates balance-sheet capacity. It releases trapped liquidity for larger-scale providers while simultaneously enforcing prudential safeguards for vulnerable entities.

5.5.3 rMLA unlocks capital investment capacity within strict thresholds

To verify that this expanded investment capacity does not compromise the viability of a provider's operations, we conduct a stress test in which all liquid assets are deployed as capital investment ($\kappa = 1$) and assess the resulting probability of a liquidity crunch. The probability of a liquidity

Table 9. Present value of incremental capital assets under the rMLA and dMLA in the baseline scenario (AUD million).

κ	MLA	**RA Heavy**	**DA Heavy**	**Large CC**	**RV Heavy**	**Small Regional**	**Expn Heavy**
0.25	rMLA	312.979	200.873	305.705	235.311	4.396	570.629
	dMLA	195.566	160.484	202.279	185.005	5.248	416.213
	Diff.	+117.413	+40.389	+103.426	+50.306	−0.852	+154.416
		(+60.04%)	(+25.17%)	(+51.13%)	(+27.19%)	(−16.23%)	(+37.10%)
0.50	rMLA	496.227	315.752	502.879	363.280	6.373	883.943
	dMLA	336.056	260.935	363.921	294.431	7.563	674.412
	Diff.	+160.171	+54.817	+138.958	+68.849	−1.190	+209.531
		(+47.66%)	(+21.01%)	(+38.18%)	(+23.38%)	(−15.73%)	(+31.07%)
0.75	rMLA	601.858	380.302	629.815	429.942	7.157	1,053.252
	dMLA	432.346	322.450	482.158	357.776	8.402	829.260
	Diff.	+169.512	+57.852	+147.657	+72.166	−1.245	+223.992
		(+39.21%)	(+17.94%)	(+30.62%)	(+20.17%)	(−14.82%)	(+27.01%)
1.00	rMLA	664.818	419.008	718.579	469.428	7.483	1,152.376
	dMLA	495.104	360.851	572.745	396.837	8.753	931.234
	Diff.	+169.714	+58.157	+145.834	+72.591	−1.270	+221.142
		(+34.28%)	(+16.12%)	(+25.46%)	(+18.29%)	(−14.51%)	(+23.75%)

Notes: The table reports the present value of increased capital assets under the rMLA and dMLA in the baseline scenario, by provider archetype and CAPEX investment rate κ. "Diff." denotes the rMLA value minus the dMLA value; a positive figure indicates that the rMLA permits a larger present value of CAPEX than the dMLA. Values in parentheses represent the relative percentage change from the dMLA baseline.

crunch under an rMLA regime is below 1% across all archetypes and scenarios (see Table 10). This result underscores the ability of this requirement to protect providers against severe shocks.

Table 10. Probability of a liquidity crunch under the maximum investment strategy ($\kappa = 1$) by provider archetype and scenario.

Archetype	**Baseline**		**Shock**	
	rMLA	dMLA	rMLA	dMLA
RA Heavy	< 0.01%	< 0.01%	< 0.01%	< 0.01%
DA Heavy	< 0.01%	< 0.01%	0.02%	< 0.01%
Large CC	< 0.01%	< 0.01%	< 0.01%	< 0.01%
RV Heavy	< 0.01%	< 0.01%	0.06%	< 0.01%
Small Regional	< 0.01%	**1.02%**	< 0.01%	**2.24%**
Expn Heavy	< 0.01%	< 0.01%	0.14%	< 0.01%

Notes: The table reports the simulated probability of a liquidity crunch for each provider archetype with the maximum CAPEX investment rate, $\kappa = 1$. Results are shown for both the baseline and shock scenarios and are compared under both the rMLA and dMLA requirements.

By contrast, the dMLA fails to provide this safety net for the Small Regional archetype. As Table 9 illustrates, the dMLA permits this archetype to sustain a high CAPEX rate and correspondingly low liquidity buffer. This occurs because the dMLA's reliance on backward-looking accounting metrics fails to capture the idiosyncratic, forward-looking tail risks that disproportionately affect smaller, less diversified providers. As a result, the Small Regional archetype faces a non-trivial liquidity crunch probability (exceeding 1%) under both baseline and shock scenarios. This contrast reflects the central design difference between the two requirements: the rMLA is constructed from forward-looking, idiosyncratic, and risk-sensitive funding burdens, whereas the dMLA's partly backward-looking and

stylised structure leaves it less effective at capturing prospective liquidity risk.

6 Policy implications

This paper establishes four policy lessons that extend beyond the Australian aged care sector.

6.1 The opportunity cost of liquidity regulation

When regulators mandate liquidity buffers, they must weigh the private opportunity costs of trapped capital against the social benefits of preventing fire sales (Roberts et al., 2023). Our findings suggest that rigid, one-size-fits-all buffers fail this cost-benefit test. By heavily penalising capital formation without formally modelling stochastic run-risk, the dMLA imposes substantial opportunity costs on aged care infrastructure investment, driving an over-accumulation of liquid assets that effectively crowds out private capital and amplifies systemic misallocation (Fueki et al., 2024). Conversely, our proposed rMLA unlocks up to AUD 223 million in capital formation for one provider, while reliably suppressing the probability of a systemic liquidity crunch to well below 1%.

6.2 Micro-prudential rules vs. macro-prudential realities

As Vives (2014) and Kara and Ozsoy (2020) demonstrate, when regulators design rules to eliminate micro-prudential (stand-alone) risk, they frequently amplify macro-prudential (systemic) vulnerabilities. The dMLA illustrates this tension: while it safeguards smaller, fragile providers, it simultaneously imposes excessive liquidity buffers on well-capitalised providers, choking off aggregate industry growth. By conditioning the liquidity constraint on actual risk-bearing capacity, our proportional rMLA resolves this tension.

However, unlike risk-sensitive banking frameworks that advocate relaxing liquidity rules for smaller institutions (Acosta-Smith et al., 2026), our rMLA dictates the reverse. This divergence stems from the distinct transmission mechanisms of systemic risk across the two sectors. In banking, the distress of a large institution can trigger an internal systemic shock through complex interbank lending and derivatives networks (Sydow et al., 2024). By contrast, the aged care sector lacks such direct network interconnectedness; it is instead exposed to external systemic shocks dictated by demographic shifts. Therefore, large aged care providers possess substantial balance-sheet capacity that absorbs idiosyncratic shocks more efficiently than smaller peers can.

6.3 Structural roots of the dMLA's design lag

The backward-looking architecture underpinning the dMLA is not unique to Australian aged care. As shown in Table 1, operating reserves in the United States (Pearson, 2006; Zarem, 2010) and escrow-based safeguards in Japan (Aveline-Dubach, 2022; Sakurai, 2017) share the same structural feature: liquidity adequacy is anchored to realised accounting flows, even though true outflows are driven by stochastic, demographic events. Yet this design lag is not a technological constraint. Adjacent APRA-regulated sectors in Australia, such as private health insurance (HPS 110, HPS 231) and

superannuation funds (SPS 530, SPG 530), already discipline analogous liquidity risks through probabilistic, scenario-based stress testing (Table 1). The persistence of accounting-based buffers in aged care therefore reflects a structural gap in regulatory maturity rather than a binding implementation barrier; the rMLA offers a transferable template to bridge this shortfall across similar jurisdictions.

6.4 Aligning with the broader trajectory of prudential regulation

The introduction outlined the parallel between our proposed rMLA and the hybrid architecture of Basel III/IV. We now develop this parallel in detail. Bank regulators initially relied on rigid, fixed-coefficient buffers (Basel I), transitioned toward purely stochastic internal models (Basel II), and ultimately converged on a hybrid framework anchored by a standardised output floor (Cummings and Durrani, 2016). The Australian aged care sector currently sits at the Basel I stage: the dMLA aggregates past expenditures and balance-sheet items through fixed coefficients, with no explicit modelling of stochastic outflows.

The rMLA proposed in this paper occupies an intermediate position analogous to the Basel III/IV equilibrium. It rests on stochastic foundations (multidimensional stress testing of resident-flow and macroeconomic risks) yet maps these foundations into a tractable linear formula in observable balance-sheet quantities. This design enables regulators to integrate risk sensitivity with the existing rule-based architecture, without requiring providers to develop bespoke internal models.

7 Conclusion

The default one-size-fits-all liquidity rules create a dual distortion in the non-bank sector: they constrain capital formation by over-buffering strong providers while leaving fragile firms exposed to systemic risk. This dual distortion is not a calibration problem but a structural one. The underlying liquidity risk of aged care providers is inherently dynamic: illiquid investments are exposed to event-driven, refundable liabilities dictated by macroeconomic and demographic shifts. A single, static percentage struggles to balance these competing demands across providers of all sizes; therefore, risk sensitivity is structurally necessary, not an optional refinement.

To establish this claim, this paper makes three contributions. First, we operationalise resident-flow risk in a form suitable for prudential calibration. The closed-form transient distribution and length-of-stay decomposition turn event-driven refundable liabilities into objects estimable from accounting data. Second, the rMLA shows that the hybrid stochastic-to-rule architecture of modern banking regulation is exportable beyond the banking perimeter. Its balance-sheet-conditioned coefficients combine the transparency of a uniform buffer with provider-specific risk sensitivity. Third, the simulation outcomes validate the advantages of the rMLA. Compared to the dMLA, it drives a structural expansion of the capital–liquidity frontier rather than a mere marginal recalibration. Additionally, the reverse direction of the proportional adjustment underscores the important parallels and distinctions between the aged care sector and the banking industry.

Beyond the Australian setting, our findings call for a paradigm shift in how regulators approach non-bank financial fragility. Decoupling liquidity rules from underlying capital dynamics does not increase safety; it undermines long-term sector sustainability. As ageing demographics increasingly

strain global capital markets, understanding how non-bank institutions manage their structural liquidity risks remains a critical frontier for financial stability research and the design of next-generation prudential frameworks.

Several caveats qualify our findings and outline avenues for future research. First, the current framework takes CAPEX investment decisions as exogenous over a one-year horizon. Second, the stress scenario is anchored to a single, extreme post-pandemic episode. Furthermore, while the aged care sector lacks direct interbank-style contagion, the setting abstracts from indirect real-economy externalities, such as local real estate fire sales or sector-wide reputational stigma. Therefore, endogenising investment strategies over a longer horizon, transitioning from a single regime shift to a regime-switching framework to account for extreme risks, and modelling these indirect spillovers are natural extensions of the present analysis.

Appendix A Resident-flow dynamics

This appendix develops a unified treatment of resident dynamics that applies to both the RA and RV settings, providing tractable expressions for the census-driven cash flows appearing in Equations (13), (14), (15), (16), and (18).

A.1 Aggregate-level risks

We model the resident census $N(t)$ within a facility of fixed capacity V as a continuous-time stochastic process on the state space $\{0, 1, \ldots, V\}$.

Assumption A.1 (Regime shift in arrivals and departures)**.**

1. *Pre-change stationary regime. The census process evolves under a capacity-blocked birth–death dynamics with admission intensity λ_0 (when $N(t) < V$) and per-resident departure hazard ν_0. The system is in statistical equilibrium at $t = 0^-$.*

2. *Regime shift at $t = 0$. At $t = 0$, the system switches to admission intensity λ and per-resident departure hazard ν (again subject to the capacity constraint V).*

Remark A.1 (Pre-change admission intensity)**.** *Let $n_0 := N(0)$ denote the realised resident census at the regime-change date $t = 0$. We calibrate λ_0 by solving*

$$n_0 = \rho_0\big(1 - B(V, \rho_0)\big)$$

for $\rho_0 = \lambda_0/\nu_0$, and then setting $\lambda_0 = \nu_0\rho_0$, where $B(V, \rho_0)$ denotes the Erlang–B blocking probability in an $M/M/V/V$ loss system (De Bruin et al., 2010). The $M/M/V/V$ structure is used here as a tractable approximation to a capacity-constrained admission process. In particular, it maps offered load ρ_0 into occupied capacity through the carried-load identity $\rho_0(1-B(V, \rho_0))$, allowing the baseline admission intensity to be pinned down from the observed census n_0 and the departure rate ν_0.

Our analysis focuses on the transient evolution for $t \geq 0$, conditioned on the realised initial census.

Definition A.1 (Generator of the census CTMC). *The process $\{N(t)\}_{t\geq 0}$ evolves as a continuous-time Markov chain (CTMC) with infinitesimal generator matrix Q (De Bruin et al., 2010), whose non-zero entries are defined by:*

$$Q_{n,n+1} = \lambda, \quad Q_{n,n-1} = n\nu, \quad Q_{n,n} = -(\lambda \mathbb{I}_{\{n<V\}} + n\nu \mathbb{I}_{\{n>0\}}),$$

where $\mathbb{I}_{\{\cdot\}}$ denotes the indicator function.

Proposition A.1 (Transient distribution of census). *Let $p(t) \in \mathbb{R}^{V+1}$ be the row vector of state probabilities with components $p_n(t) := Pr(N(t) = n \mid N(0) = n_0)$. The transient distribution is given by the matrix exponential (Moler and Van Loan, 2003):*

$$p(t) = e_{n_0}^{\top} e^{Qt}, \tag{24}$$

where e_{n_0} is the standard basis vector with unity at index n_0.

This representation delivers tractable expressions for the aggregate resident risks entering Equations (13), (14), and (16).

Remark A.2 (Occupancy approximation). *If admissions decrease, departures increase, and capacity blocking is negligible, then conditional on $N(0) = n_0$, the expected occupancy rate at time $t = 1$ can be approximated by $\omega \left(e^{-\nu} + \frac{\lambda}{n_0 \nu}(1 - e^{-\nu})\right)$, where ω denotes the initial occupancy rate.*

We next characterise admissions over $[t, t + \Delta t)$ as a marked transition functional of the CTMC.

Definition A.2 (Admission count and upward-transition operator). *Let $\Delta A(t)$ denote the number of admissions over $[t, t + \Delta t)$. Define $Q^+ \in \mathbb{R}^{(V+1)\times(V+1)}$ by*

$$(Q^+)_{i,i+1} = \lambda \mathbb{I}_{\{i<V\}}, \qquad (Q^+)_{i,j} = 0 \text{ otherwise},$$

and let $\mathbf{1}$ be the all-ones column vector in $\mathbb{R}^{V+1}$.

Proposition A.2 (Conditional probability generating function of admissions). *For any $n \in \{0, 1, \ldots, V\}$, the conditional probability generating function of $\Delta A(t)$ satisfies*

$$G_{A|n}(z) := \mathbb{E}\left[z^{\Delta A(t)} \mid N(t) = n\right] = e_n^{\top} \exp\Big((Q + (z-1)Q^+)\Delta t\Big)\mathbf{1}. \tag{25}$$

Moreover, the conditional mass function is obtained by coefficient extraction:

$$\mathbb{P}(\Delta A(t) = a \mid N(t) = n) = \frac{1}{a!} \frac{\partial^a}{\partial z^a} G_{A|n}(z)\Big|_{z=0}, \qquad a = 0, 1, 2, \ldots. \tag{26}$$

This proposition yields tractable admission-risk expressions for Equation (15).

A.2 Individual-level risks

Because loan refunds and retention are tenure-dependent, aggregate cash outflows and liability relief cannot be characterised solely by aggregate stocks without tracking the distribution of LOS among

RA and RV payers. We therefore model the refundable loan as a deposit-type liability with withdrawal risk and model retention at the individual level. We characterise resident heterogeneity by elapsed LOS $\ell \geq 0$ at time t.

Lemma A.1 (Snapshot LOS density)**.** *Let $f^{in}(\ell; t)$ denote the density of elapsed LOS among residents present at time t. It is a mixture of two cohorts: (i) incumbents already in care at $t = 0$, whose pre-change elapsed-LOS distribution is the stationary age distribution implied by the pre-change departure hazard ν_0; and (ii) post-change entrants admitted over $(0, t]$ at effective intensity $\lambda[1-p_V(s)]$ and surviving to time t under the post-change hazard ν. Then*

$$f^{in}(\ell; t) = \frac{1}{Z(t)} \left[\mathbb{I}_{\{0 \leq \ell < t\}} \lambda (1 - p_V(t - \ell))\, e^{-\nu \ell} + \mathbb{I}_{\{\ell \geq t\}} \left(n_0 e^{-\nu t} \right) \nu_0 e^{-\nu_0 (\ell - t)} \right], \tag{27}$$

where

$$Z(t) = \int_0^t \lambda \left[1 - p_V(t - u)\right] e^{-\nu u}\, du + n_0 e^{-\nu t}.$$

Proof. Decompose residents present at time t into post-change entrants and incumbents. For $\ell < t$, the resident must have entered at time $t - \ell$, with effective admission intensity $\lambda(1 - p_V(t - \ell))$, and survived for ℓ periods under hazard ν, giving $\mathbb{I}_{\{0 \leq \ell < t\}} \lambda(1 - p_V(t - \ell)) e^{-\nu \ell}$. For $\ell \geq t$, the resident must be an incumbent present at $t = 0$. The surviving incumbent mass at time t is $n_0 e^{-\nu t}$, and the pre-change elapsed-LOS density is $\nu_0 e^{-\nu_0 (\ell - t)}$, giving $\mathbb{I}_{\{\ell \geq t\}} (n_0 e^{-\nu t}) \nu_0 e^{-\nu_0 (\ell - t)}$. Adding the two terms gives the unnormalised density, and normalising by $Z(t)$ yields Equation (27). □

Lemma A.1 provides the within-facility LOS composition needed to aggregate tenure-dependent retention and refund cash flows. We next derive moment generating functions (MGFs) for aggregate retention and refunds over $[t, t + \Delta t)$, conditional on the realised census $N(t) = n$. Let $g(\ell) \in [0, 1]$ denote the non-increasing refund schedule.

Refunds and retention are triggered by departures. Under the exponential LOS benchmark, departures over a short interval are independent conditional on the census.

Lemma A.2 (Departures over a discrete interval)**.** *Conditional on $N(t) = n$, each resident departs over $[t, t + \Delta t)$ independently with probability*

$$q(\Delta t) = 1 - e^{-\nu \Delta t},$$

and hence

$$\Delta D(t) \mid N(t) = n \sim \mathit{Bin}(n,\ q(\Delta t))\,. \tag{28}$$

Because the post-change hazard is constant, conditioning on departure does not tilt the LOS composition among departures relative to those in care, i.e., $f^{\text{dep}}(\ell; t) \equiv f^{\text{in}}(\ell; t)$ (independent thinning; Eick et al., 1993). This yields a closed-form conditional MGF for total refunds.

Proposition A.3 (Conditional MGF of total refunds)**.** *Conditional on $N(t) = n$, the MGF of total refunds over $[t, t + \Delta t)$ in Equation (18) is*

$$M_{O^{out} | N(t) = n}(s) = \left(1 - q(\Delta t) + q(\Delta t)\, M_{\tilde{Y}^{out}}(s)\right)^n, \tag{29}$$

where $M_{\tilde{Y}^{out}}(s)$ is the MGF of a single refund conditional on departure:

$$M_{\tilde{Y}^{out}}(s) = 1 - \Pr(\cdot) + \Pr(\cdot) \int_0^\infty \exp\Big\{ s\, g(\ell)\, P^{in} \Big\}\, f^{in}(\ell; t)\, d\ell. \tag{30}$$

For the RV case, $\Pr(\cdot) = 1$*; for the RA case,* $\Pr(\cdot) = \theta_{RA}$*.*

Proposition A.4 (Conditional MGF of total retention)**.** *Conditional on $N(t) = n$, the MGF of the RA/RV retention in Equation (10) or (11) over $[t, t + \Delta t)$ is*

$$M_{L_{ret}|N(t)=n}(s) = \left(1 - q(\Delta t) + q(\Delta t)\, M_{\tilde{Y}^{ret}}(s)\right)^n, \tag{31}$$

where the single-resident MGF accounts for payment-type mixing:

$$M_{\tilde{Y}^{ret}}(s) = 1 - \Pr(\cdot) + \Pr(\cdot) \int_0^\infty \exp\Big\{ s\, [1 - g(\ell)]\, P^{in} \Big\}\, f^{in}(\ell; t)\, d\ell. \tag{32}$$

Appendix B Calibration

B.1 Calibration of archetype balance sheet

This subsection describes the calibration of selected archetype-specific parameters reported in Table 6. To improve clarity, the calibration procedure is structured as follows:

- Probability of choosing RA (θ_{RA}): For each archetype, the probability that a newly admitted resident opts for a refundable accommodation deposit is set in a way such that higher government subsidies per resident correlate with lower resident fee income. At the same time, this probability ensures that the implied average resident fee strictly exceeds the annualised basic daily fee.

- Daily accommodation payment (P_{DA}): The average daily accommodation payment per resident is linked to the per-resident incoming RA loan amount, $P^{\text{in}}_{\text{RA}}$, through the standard industry relationship $P_{\text{DA}} = 7.65\% P^{\text{in}}_{\text{RA}}$ (StewartBrown, 2025a).

- Incoming refundable loan amounts ($P^{\text{in}}_{\text{RA}}$ and $P^{\text{in}}_{\text{RV}}$): The per-resident RA loan amount, $P^{\text{in}}_{\text{RA}}$, is estimated as the current per-resident RA liability plus half of the maximum retention amount. This adjustment is necessary because financial statements report liabilities net of accrued retention deductions; by adding back half of the maximum retention cap (i.e., 5% for RA and 15% for RV), we proxy the gross initial loan amount by assuming the average incumbent resident is halfway through their retention cycle. The same convention is used when constructing the corresponding per-resident RV loan amount.

- Resident fees (F^{RACF} and F^{RV}): The average RACF resident fee, F^{RACF}, is derived residually. From total operating revenue, excluding retained loan amounts, we subtract government subsidies, estimated RV fee revenue, and DA revenue. The remaining amount is attributed to RACF resident fees and is then divided by the RACF census (n^{RACF}). For the RV segment, we assume an annual recurrent fee of $\$7,000$ per resident.

- Fixed operating expenses (O^{other}): Finally, unlike the other revenue and expense items, O^{other} is not expressed on a per-resident basis, but is treated as the residual component of expenses that does not scale directly with the census.

B.2 Rationale for stress dimensions

On the occupancy side, we reduce admissions to $0.85\lambda_0$ and increase the per resident departure rate to $1.15\nu_0$ for both RACF and RV in the extreme scenario. According to Remark A.2, the RACF resident census declines by approximately 7.7% over the one-year horizon. By contrast, because ν_0^{RACF} and ν_0^{RV} differ, the corresponding decline for RV is about 3%. Considering the design of the dMLA, with a 2% buffer for RV loan and a 10% buffer for RA liabilities, we view this calibration as reasonable.

On the economic side, we implement the scenario using a conditional VAR(p) forecast augmented with a one-off structural inflation shock that captures the post-COVID inflation regime and the ACQSC's "higher inflation" environment.[16] Specifically, the macro state vector follows

$$(\pi_t, r_t)^\intercal = c + \sum_{j=1}^{p} A_j(\pi_{t-j}, r_{t-j})^\intercal + u_t, \qquad u_t = H\varepsilon_t, \qquad \varepsilon_t \sim \mathcal{N}(0, I). \tag{33}$$

The matrix H is the contemporaneous impact matrix (implemented as a Cholesky factor in our baseline specification), implying $\Sigma \equiv \text{Var}\,(u_t) = HH^\top$. Hence, simulating $\varepsilon_t \sim \mathcal{N}(0, I)$ and mapping $u_t = H\varepsilon_t$ reproduces the empirical contemporaneous covariance structure of reduced-form innovations. Figure 4 reports the implied paths of inflation and the nominal interest rate under the baseline and shock scenarios.

Regarding the remaining two dimensions, we first assume the excess return on short-term liquid placements is reduced to zero. This ensures the short-term investment rate strictly coincides with the nominal risk-free rate, capturing a typical flight-to-liquidity dynamic wherein severe market stress systematically eliminates the premium on yield-bearing assets (Acharya et al., 2013). Second, we perturb the term-structure inversion threshold, defined as the minimum leverage ratio at which the short-term debt rate exceeds its long-term counterpart. This inversion occurs when the multiplier $\exp\left(\phi_1 + \phi_2 \frac{L(t)}{X(t)}\right)$ from Equation (9) surpasses unity. We compress this threshold from 0.7 in the baseline to 0.3 under the shock. This reduction reflects how intensifying rollover risk during downturns triggers inverted funding costs at progressively lower leverage levels (Chen et al., 2021), an effect further amplified by heightened spread sensitivity to institutional performance under extreme stress (Wang et al., 2020).

B.3 Sensitivity analysis

We conduct a one-dimensional sensitivity analysis of dMLA breach probability and the minimum buffer rate defined in Section 5.3. Starting from the unstressed baseline, we vary one stress dimension at a time to its mild, shock, or extreme level, as reported in Table 11, while holding the remaining

[16] This specific temporal window captures a macroeconomic phase wherein nominal interest rates remained low while inflationary pressures escalated, triggering a material cost–revenue squeeze for providers.

three dimensions at their baseline values. For each of the six provider archetypes, we examine two outcomes: (i) the change in dMLA breach probability at $\kappa = 1$; and (ii) the change in the minimum buffer rate, both measured relative to the unstressed baseline. The corresponding results are shown in Figure 12.

Table 11. Extended stress scenarios for sensitivity analysis.

Scenario	$\Delta\pi(0)$	λ	ν	$\Delta\delta_1$	$\Delta\phi_1$	$\Delta\phi_2$
Mild	1%	$0.9\lambda_0$	$1.1\,\nu_0$	-0.25%	0.120	0.020
Shock	1.3%	$0.85\lambda_0$	$1.15\,\nu_0$	-0.5%	0.125	0.025
Extreme	1.6%	$0.8\lambda_0$	$1.2\,\nu_0$	-0.75%	0.130	0.030

Notes: The extended stress scenarios are parameterised along four stress dimensions: (1) the initial inflation shock, $\Delta\pi(0)$; (2) resident-flow dynamics, captured jointly by the admission rate λ and departure hazard ν; (3) the change in excess return, $\Delta\delta_1$; and (4) borrowing conditions, captured by $\Delta\phi_1$ and $\Delta\phi_2$.

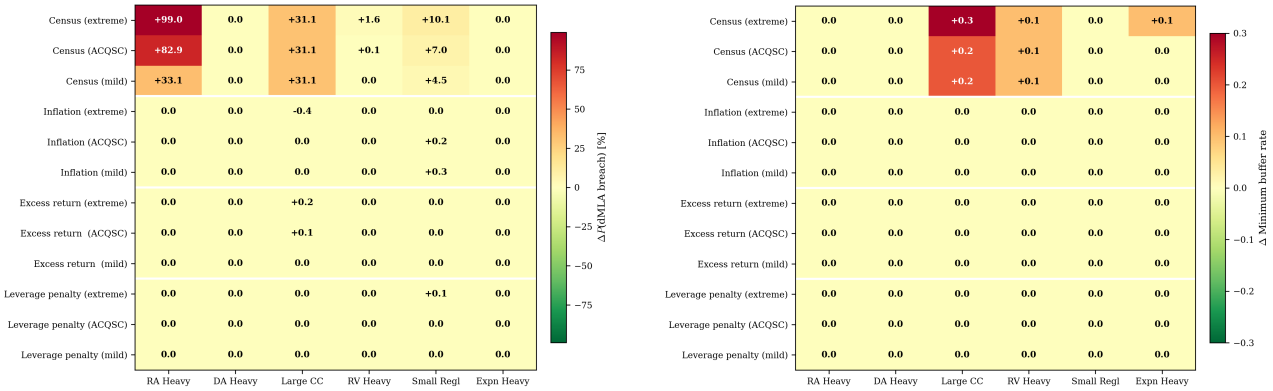

(a) Changes in dMLA breach probability ($\kappa = 1$). **(b)** Changes in minimum buffer rate.

Figure 12. One-dimensional sensitivity analysis: changes in dMLA breach probability and the minimum initial buffer rate relative to the baseline under alternative stress dimensions.

Figure 12(a) shows that the resident-flow dimension is the main driver of changes in dMLA breach probability. By contrast, the inflation dimension has a more nuanced effect. Higher inflation raises expenditures and, under our assumptions, government subsidies do not adjust correspondingly, which increases liquidity pressure. However, when inflation exceeds the nominal interest rate, the real borrowing burden declines, partly offsetting this adverse effect and making CAPEX relatively more attractive. As a result, a more severe inflation shock does not always produce a materially larger increase in dMLA breach probability. Furthermore, Figure 12(b) shows that changes in the minimum initial buffer rate are also most sensitive to the resident-flow dimension, indicating that adverse admission and departure dynamics are the primary determinant of the additional liquidity buffer required under stress.

Appendix C Details on the rMLA

C.1 Generation of the synthetic providers

Let $K = 6$ denote the number of provider archetypes described in Section 4.1, and let $\xi_k \in \mathbb{R}^d$, with $d = 24$, denote the vector of operational and balance sheet items characterising archetype k

$(k = 1, \ldots, K)$ within the stochastic simulation framework of Section 3. We assume that aged care providers in the market may exhibit operating characteristics lying within, or close to, the range spanned by these archetypes. For a generic synthetic provider, the corresponding vector of items ξ is given by the convex combination

$$\xi \;=\; \sum_{k=1}^{K} w_k\, \xi_k, \qquad \text{with } \sum_{k=1}^{K} w_k = 1, \quad w_k \geq 0.$$

For the analysis of the liquidity requirements, we generate $M = 5{,}000$ synthetic providers indexed by $j = 1, \ldots, M$. The baseline weight vector $\mathbf{w}_j = (w_{j,1}, \ldots, w_{j,K})^\top$ for provider j is drawn independently from a symmetric Dirichlet distribution, $\mathbf{w}_j \sim \mathrm{Dir}(\mathbf{1}_K)$. The Dirichlet distribution is the standard probability distribution on the K-dimensional simplex, that is, on the set of vectors $\mathbf{w} \in [0,1]^K$ satisfying $\sum_{k=1}^{K} w_k = 1$; with concentration parameter $\mathbf{1}_K$ it reduces to the uniform distribution over this simplex.

To allow synthetic providers to fall slightly outside the convex combination of the archetypes while preserving realistic scenarios, each baseline weight is perturbed by an independent additive Gaussian noise term:

$$\tilde{w}_{j,k} \;=\; w_{j,k} + \epsilon_{j,k}, \qquad \epsilon_{j,k} \overset{\text{i.i.d.}}{\sim} \mathcal{N}\Big(0,\, m^2/K\Big), \qquad k = 1, \ldots, K,$$

where $m \geq 0$ controls the extrapolation margin. The perturbed weights are then truncated below at $-m$ (with $m = 0.1$) and renormalised as

$$w^*_{j,k} \;=\; \frac{\max(\tilde{w}_{j,k},\, -m)}{\sum_{l=1}^{K} \max(\tilde{w}_{j,l},\, -m)}, \qquad k = 1, \ldots, K.$$

By construction the resulting weights satisfy $\sum_{k=1}^{K} w^*_{j,k} = 1$ but are no longer constrained to be non-negative, so each synthetic provider may lie just outside the simplex spanned by the archetypes. The synthetic vector of items for provider j is then

$$\xi^*_j \;=\; \sum_{k=1}^{K} w^*_{j,k}\, \xi_k, \qquad j = 1, \ldots, M.$$

To guarantee that every synthetic vector ξ^*_j translates into a structurally operable provider, we enforce the following post-processing on the blended outputs:

- *Indivisibility:* Variables denoting physical counts (e.g., bed capacity, initial resident populations, arrival rates) are rounded to non-negative integers.
- *Probability conservation:* Payment choice probabilities are bounded to $[0, 1]$ and normalised such that $\theta_{\mathrm{RA}} + \theta_{\mathrm{DA}} = 1$.
- *Capacity bounds:* Simulated initial occupancies are capped so as not to exceed the simulated physical bed capacity.

We stress that the synthetic sample is risk-based rather than prevalence-based: the symmetric

Dirichlet weighting places equal density on every admissible configuration and is not meant to reproduce the empirical market shares of the six provider types. This mirrors the usual role of archetypes in prudential regulation, where stylised firms calibrate a standardised formula and span the outcomes it must withstand, rather than describe the current industry composition.

Figure 13 shows the first two principal components for the balance sheet and operational items (explaining a total of 99.4% of the total variation) of the synthetic aged care providers.

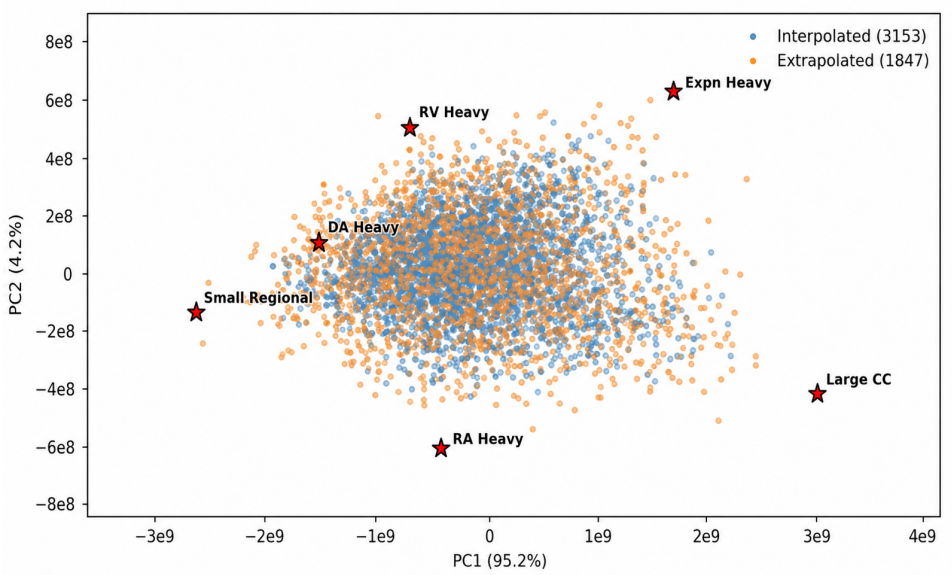

Figure 13. Principal component projection onto the first two components of the space of synthetic providers.

The coefficients of Equation (22) are then estimated by ridge regression of $\{B_j^\star\}_{j=1}^M$ on the five standardised balance-sheet covariates $\widetilde{x}_j$ defined in Equation (34):

$$\hat{\boldsymbol{\beta}} \;=\; \arg\min_{\boldsymbol{\beta}} \sum_{j=1}^{M} \left(B_j^\star - \beta_0 - \sum_{i=1}^{5} \beta_i \, \widetilde{x}_{i,j} \right)^2 + \lambda \|\boldsymbol{\beta}\|_2^2,$$

with the penalty parameter λ selected by 5-fold cross-validation over a logarithmically spaced grid of 50 candidate values, $\lambda \in \{10^{-3}, 10^{-3+6/49}, \ldots, 10^{3}\}$; for each candidate the average held-out mean squared error across the five folds is computed, and the value $\lambda^\star$ minimising this criterion is retained to re-estimate the coefficients on the full sample of $M = 5{,}000$ synthetic providers. The ridge penalty addresses the partial collinearity that arises because the synthetic sample is generated from only $K = 6$ underlying archetypes; in practice the cross-validated penalty is small ($\lambda^\star \approx 0.022$), indicating only mild shrinkage relative to ordinary least squares. The estimated coefficients $\hat{\boldsymbol{\beta}}$, together with the sample moments needed to convert them into the unstandardised form of Equation (23), are reported in Table 12 and further discussed in Appendix C.2.

Table 12. Standardised regression coefficients and sample moments of the covariates.

Standardised covariate	$\hat{\beta}$	Mean	Standard deviation
$\widetilde{X^c/X^l}$	−0.805	12.548	2.353
$\widetilde{X^r/X^l}$	0.225	0.179	0.055
$\widetilde{L^s/X^l}$	0.484	1.688	0.341
$\widetilde{L^l/X^l}$	0.119	1.329	0.482
$\widetilde{L^{\mathrm{RA}}/X^l}$	0.178	7.514	2.177

Notes: All covariates are first expressed as ratios to initial liquid assets X^l and then standardised as in (34) prior to estimation. The estimated intercept is 0.131 and the model attains an R^2 of 0.792. The cross-validated ridge penalty is 0.022, indicating only mild collinearity among the regressors.

C.2 Derivation of the buffer-rule specification

To eliminate scale effects and to facilitate comparison across providers of different sizes, we divide all variables by the benchmark quantity X^l:

$$B^\star = \frac{\mathcal{B}}{X^l}, \quad x_1 = \frac{X^c}{X^l}, \quad x_2 = \frac{X^r}{X^l}, \quad x_3 = \frac{L^s}{X^l}, \quad x_4 = \frac{L^l}{X^l}, \quad x_5 = \frac{L^{\mathrm{RA}}}{X^l},$$

where $\mathcal{B}$ denotes the simulated minimum buffer level. The following model is estimated:

$$B^\star = \beta_0 + \sum_{j=1}^{5} \beta_j \widetilde{x_j}, \qquad \widetilde{x_j} = \frac{x_j - \mu_j}{\sigma_j}, \tag{34}$$

where each covariate $\widetilde{x_j}$ is centred and scaled by its sample mean μ_j and sample standard deviation σ_j, while the dependent variable is retained on its original scale. This formulation is convenient for estimation and measurement of the relative importance of the covariates. For a meaningful economic interpretation of the effect of the covariates we recast (34) in unstandardised form,

$$B^\star = \alpha_0 + \sum_{j=1}^{5} \alpha_j x_j, \tag{35}$$

where the regression coefficients have been recalculated as

$$\alpha_j = \frac{\beta_j}{\sigma_j}, \qquad \alpha_0 = \beta_0 - \sum_{j=1}^{5} \alpha_j \mu_j. \tag{36}$$

The estimates of (34), together with the sample moments required for the de-standardisation in (36), are shown in Table 12. Each standardised coefficient measures the change in the minimum buffer rate associated with a one-standard-deviation increase in the corresponding regressor.[17]

Multiplying both sides of (35) by the benchmark quantity X^l yields a closed-form expression for

[17] We do not report significance levels, as the data are synthetically generated; given a sufficiently large simulated sample, every regressor would eventually appear statistically significant.

the buffer level in terms of the original, unnormalised variables,

$$\mathcal{B} = \alpha_0 X^l + \alpha_1 X^c + \alpha_2 X^r + \alpha_3 L^s + \alpha_4 L^l + \alpha_5 L^{\mathrm{RA}}, \tag{37}$$

which is precisely the specification adopted in Equation (23).

C.3 Robustness test of rMLA

Figure 14 presents the sensitivity of the fitted rMLA coefficients to the choice of short-term repayment horizon. The left panel plots the estimated coefficient on each balance-sheet covariate across horizons of four to ten months; the right panel expresses each coefficient as a ratio relative to the seven-month baseline, isolating the proportional deviation attributable to horizon choice.

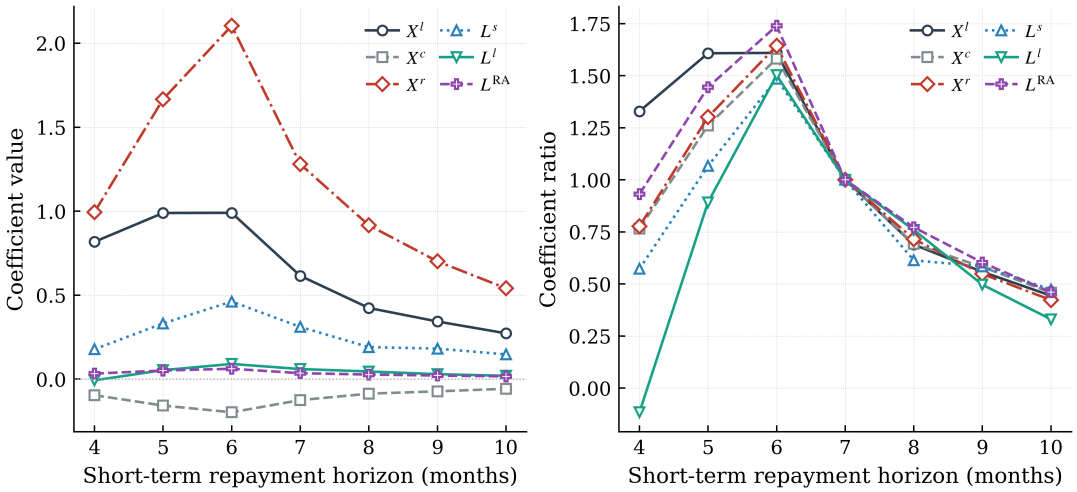

Figure 14. Sensitivity of fitted rMLA coefficients to the short-term repayment horizon. The left panel reports the estimated coefficient on each balance-sheet covariate across repayment horizons of 4–10 months. The right panel expresses each coefficient as a ratio relative to the baseline horizon of seven months, isolating the proportional deviation attributable to horizon choice.

The right panel reveals two distinct regimes. For horizons of eight to ten months, lengthening the repayment window beyond the baseline uniformly reduces the minimum buffer requirement, with the fitted coefficients contracting in broadly equal proportions across covariates. A symmetric pattern emerges when the horizon is shortened to six months: all coefficients rise by comparable magnitudes, implying a commensurately higher minimum buffer. Across this range, the adjustment is well characterised as a near-homogeneous rescaling of the baseline formula.

For horizons of four and five months, however, the coefficient ratios diverge from this proportional pattern, indicating that a common rescaling no longer provides an adequate approximation. Notably, the contribution of short-term debt increases by less than might be expected, while long-term debt remains a modest loading throughout. This is not fully consistent with the intuition that a shorter repayment horizon should disproportionately amplify the role of short-term liabilities. The underlying reason is that varying the repayment horizon does not materially alter the provider's aggregate repayment burden over the one-year stress window; rather, it shifts the timing pressure on near-term cash flows. Consequently, the fitted rMLA depends primarily on overall balance-sheet capacity and

refund-related exposure, rather than on the short-term debt coefficient L^s alone.

CRediT authorship contribution statement

Lingfeng Lyu: Conceptualization, Data curation, Formal analysis, Investigation, Methodology, Software, Supervision, Validation, Visualization, Writing – original draft, Writing – review & editing.

Michael Sherris: Conceptualization, Funding acquisition, Investigation, Methodology, Project administration, Resources, Supervision, Writing – original draft, Writing – review & editing.

Francesco Ungolo: Methodology, Supervision, Writing – original draft, Writing – review & editing.

Zhiqian Ye: Conceptualization, Data curation, Formal analysis, Investigation, Methodology, Software, Validation, Visualization, Writing – original draft.

Acknowledgements

This work was supported by the Centre for Population Ageing Research (CEPAR) at UNSW Sydney through a grant from the Department of Health, Disability and Ageing(DHDA), and by the Innovations in Risk, Insurance and Superannuation (IRIS) Knowledge Hub at the UNSW Business School through a Summer Scholarship. The authors acknowledge the use of the computational cluster Katana, supported by Research Technology Services at UNSW Sydney, which contributed to the research results reported within this paper.

Declaration of generative AI and AI-assisted technologies in the manuscript preparation process

During the preparation of this work, the authors used Gemini to improve readability and language quality. After using this tool/service, the author(s) reviewed and edited the content as needed and take(s) full responsibility for the content of the published article.

Bibliography

Acharya, V. V., Amihud, Y., and Bharath, S. T. (2013). Liquidity risk of corporate bond returns: Conditional approach. *Journal of Financial Economics*, 110(2):358–386.

Acharya, V. V., Gale, D., and Yorulmazer, T. (2011). Rollover risk and market freezes. *The Journal of Finance*, 66(4):1177–1209.

Acosta-Smith, J., Arnould, G., De-Ramon, S. J., Milonas, K., and Vo, Q.-A. (2026). Capital and liquidity interaction in banking. *Journal of Financial Stability*, page 101515.

ACQSC (2025). *Financial and Prudential Standards: Guidance for Providers*. Australian Government, Canberra.

APRA (2026). Prudential handbook. Available at: https://handbook.apra.gov.au/ (accessed 10 April 2026).

Aveline-Dubach, N. (2022). Financializing nursing homes? The uneven development of Health Care REITs in France, the United Kingdom and Japan. *Environment and Planning A: Economy and Space*, 54(5):984–1004.

Brunnermeier, M. K. and Pedersen, L. H. (2009). Market liquidity and funding liquidity. *The Review of Financial Studies*, 22(6):2201–2238.

Chen, H., Xu, Y., and Yang, J. (2021). Systematic risk, debt maturity, and the term structure of credit spreads. *Journal of Financial Economics*, 139(3):770–799.

Cornett, M. M., McNutt, J. J., Strahan, P. E., and Tehranian, H. (2011). Liquidity risk management and credit supply in the financial crisis. *Journal of Financial Economics*, 101:297–312.

Cummings, J. R. and Durrani, K. J. (2016). Effect of the Basel Accord capital requirements on the loan-loss provisioning practices of Australian banks. *Journal of Banking & Finance*, 67:23–36.

Davydov, D., Vähämaa, S., and Yasar, S. (2021). Bank liquidity creation and systemic risk. *Journal of Banking & Finance*, 123:106031.

De Bruin, A. M., Bekker, R., Van Zanten, L., and Koole, G. M. (2010). Dimensioning hospital wards using the Erlang loss model. *Annals of Operations Research*, 178(1):23–43.

DHDA (2024). *Financial Report on the Australian Aged Care Sector: 2023-24*. Australian Government, Canberra.

Diamond, D. W. and Dybvig, P. H. (1983). Bank runs, deposit insurance, and liquidity. *Journal of Political Economy*, 91(3):401–419.

Donaldson, J. R., Gromb, D., and Piacentino, G. (2020). The paradox of pledgeability. *Journal of Financial Economics*, 137(2):591–605.

Eick, S. G., Massey, W. A., and Whitt, W. (1993). The physics of the M(t)/g/∞ queue. *Operations Research*, 41(4):731–742.

Fueki, T., Hürtgen, P., and Walker, T. B. (2024). Zero-risk weights and capital misallocation. *Journal of Financial Stability*, 72:101264.

Goldstein, I. and Pauzner, A. (2005). Demand–deposit contracts and the probability of bank runs. *The Journal of Finance*, 60(3):1293–1327.

Hastie, T., Friedman, J., and Tibshirani, R. (2001). *The Elements of Statistical Learning: Data Mining, Inference, and Prediction*. Springer Series in Statistics. Springer, 1 edition.

Holmström, B. and Tirole, J. (1998). Private and public supply of liquidity. *Journal of Political Economy*, 106(1):1–40.

Jiang, E. X., Matvos, G., Piskorski, T., and Seru, A. (2024). Monetary tightening and US bank fragility in 2023: Mark-to-market losses and uninsured depositor runs? *Journal of Financial Economics*, 159:103899.

Kara, G. I. and Ozsoy, S. M. (2020). Bank regulation under fire sale externalities. *The Review of Financial Studies*, 33(6):2554–2584.

Lyu, L., Shen, Y., Sherris, M., and Ziveyi, J. (2026). Financing aged care with home equity allowing for government age pension and aged care support. *Insurance: Mathematics and Economics*, page 103193.

Moler, C. and Van Loan, C. (2003). Nineteen dubious ways to compute the exponential of a matrix, twenty-five years later. *SIAM Review*, 45(1):3–49.

Pearson, K. C. (2006). Continuing care retirement communities, state regulation and the growing importance of counsel for residents and their families. *Pennsylvania Bar Association Quarterly*, 77:172–183.

RBA (2026). Statistics. Available at: https://www.rba.gov.au/statistics/ (accessed 14 January 2026).

Roberts, D. T., Sarkar, A., and Shachar, O. (2023). Liquidity regulations, bank lending and fire-sale risk. *Journal of Banking & Finance*, 156:107007.

Sakurai, T. (2017). An examination of no refund clauses in For Profit Nursing Home Contracts. *Tokyo Keizai Law Review*, 37:29–74.

Sims, C. A. (1980). Macroeconomics and reality. *Econometrica*, 48(1):1–48.

StewartBrown (2025a). *Aged Care Financial Performance Survey Report: June 2025*. StewartBrown Chartered Accountants, Sydney.

StewartBrown (2025b). *Retirement Living Performance Survey Report: FY24 results*. StewartBrown Chartered Accountants, Sydney.

Sydow, M., Schilte, A., Covi, G., Deipenbrock, M., Del Vecchio, L., Fiedor, P., Fukker, G., Gehrend, M., Gourdel, R., Grassi, A., et al. (2024). Shock amplification in an interconnected financial system of banks and investment funds. *Journal of Financial Stability*, 71:101234.

Vives, X. (2014). Strategic complementarity, fragility, and regulation. *The Review of Financial Studies*, 27(12):3547–3592.

Wang, C.-W., Chiu, W.-C., and King, T.-H. D. (2020). Debt maturity and the cost of bank loans. *Journal of Banking & Finance*, 112:105235.

Wells, A. (2024). Once in a generation aged care reforms. Available at: https://www.health.gov.au/ministers/the-hon-anika-wells-mp/media/once-in-a-generation-aged-care-reforms?language=en (accessed 24 February 2026).

Zarem, J. E. (2010). *Today's Continuing Care Retirement Community (CCRC)*. CCRC Task Force, American Seniors Housing Association, Washington, DC.